

1 The enigmatic curvature of Central Iberia and its puzzling kinematics

2 Daniel Pastor-Galán^{1,2,3}, Gabriel Gutiérrez-Alonso^{4,5}, Arlo B. Weil⁶

3

4 ¹Frontier Research Institute for Interdisciplinary Sciences, Tohoku University

5 ²Department of Earth Science, Tohoku University

6 ³Center for Northeast Asian Studies, Tohoku University, 41 Kawauchi, Aoba-ku, Sendai, 980-
7 8576, Japan. pastor.galan.daniel.a8@tohoku.ac.jp

8 ⁴Dept. of Geology. Faculty of Sciences. University of Salamanca. Plaza de la Merced s/n.
9 38007, Salamanca (Spain). gabi@usal.es

10 ⁵Geology and Geography Department, Tomsk State University, Lenin Street, 36, Tomsk 634050
11 Russia

12 ⁶Department of Geology, Bryn Mawr College, PA, USA 19010

13

14 Abstract

15 The collision between Gondwana and Laurussia that formed the latest supercontinent,
16 Pangea, occurred during Devonian to Early Permian times and resulted in a large-scale orogeny
17 that today transects Europe, northwest Africa and eastern North America. This orogen is
18 characterized by an 'S' shaped corrugated geometry in Iberia. The northern curve of the
19 corrugation is the well-known and studied Cantabrian (or Ibero-Armorican) Orocline and is
20 convex to the east and towards the hinterland. Largely ignored for decades, the geometry and
21 kinematics of the southern curvature, known as the Central Iberian curve, are still ambiguous
22 and hotly debated. Despite the paucity of data, the enigmatic Central Iberian curvature has
23 inspired a variety of kinematic models that attempt to explain its formation with little consensus.
24 This paper presents the advances and milestones in our understanding of the geometry and
25 kinematics of the Central Iberian curve from the last decade, with particular attention to
26 structural and paleomagnetic studies.

27 When combined, the currently available datasets suggest that the Central Iberian curve
28 did not undergo regional differential vertical-axis rotations during or after the latest stages of the
29 Variscan orogeny, and did not form as the consequence of a single process. Instead, its core is
30 likely a primary curve (i.e. inherited from previous physiographic features of the Iberian crust)
31 whereas the curvature in areas outside the core are dominated by folding interference during
32 the Variscan orogeny or more recent Cenozoic (Alpine) tectonic events.

33 **Keywords**

34 **Central Iberia Curve, Variscan orogen, Iberia, Cantabrian Orocline, Curved orogens,**

35 **Pangea**

36

37

38 1 Introduction

39 Mountain belt systems are the most striking product of plate tectonics. In addition to their
40 astonishing visual impact, marking the locations where ancient and modern plates collided,
41 orogenic belts often preserve a variety of rocks that have the potential to illuminate the entirety
42 of the systems pre- and syn-orogenic histories. One of the striking characteristics of most of
43 Earth's orogens are their curvature in plan-view (e.g. van der Voo, 2004; Marshak, 2004;
44 Rosenbaum, 2014). The degree of orogenic curvature may range from a few degrees of
45 deflection in structural trend (e.g. Kopet Dag, Iran), to 180° of arc curvature (e.g. Kazakhstan arc
46 and the Carpathians). The kinematics, structural and geodynamic implications of these systems
47 are as varied as their geometries (Marshak, 2004; Weil and Sussman, 2004; Johnston et al.,
48 2013). For example, some orogenic curvatures are hypothesized to be the consequence of
49 physiographic features of the basement that pre-date orogen formation, such as irregular basin
50 architectures or plate margin salients and recesses that formed from rift-to-drift processes (e.g.
51 Jura mountains, Hindle et al., 2000), which then control the growth geometry of the ensuing
52 orogen. These systems are known as primary arcs, and reflect pre-orogenic geometries and
53 show no significant or systematic vertical-axis rotations along their structural length. On the
54 other hand, oroclines, as classically defined by Carey in 1956, involve systematic differential
55 vertical-axis rotations subsequent to initial orogenic shortening: different sectors of an orogen
56 rotate with variable magnitudes or in opposite directions (e.g. Li et al., 2012). Rotations in
57 oroclines may occur at a range of scales, from thrust emplacement at upper crustal levels (e.g.
58 Izquierdo-Llavall et al., 2018), up to lithospheric-scale vertical-axis folding (e.g. Li et al., 2018).
59 They can occur as single curves (e.g. Maffione et al., 2009), coupled curves (Johnston, 2001),
60 or in trains of curves (Li and Rosenbaum, 2014). Oroclines can form during the main orogenic
61 building event, known as progressive oroclines (Johnston et al., 2013; e.g., the Wyoming
62 salient, Yonkee and Weil, 2010, and Weil et al., 2010), or during a subsequent tectonic pulse,
63 so-called secondary oroclines (Weil and Sussman, 2004). Unraveling the kinematics and
64 mechanisms of curvature formation in mountain belts is a critical step to understanding
65 orogenesis in 4D and to evaluate their geodynamic consequences and paleogeographic
66 implications.

67 The Variscan-Alleghanian orogeny resulted in the suturing of Gondwana and Laurussia
68 during Devonian-Carboniferous times, and ultimately led to the formation of the supercontinent,
69 Pangea. This long and sinuous orogen runs for >8000 km along strike and is ca. 1000 km wide,
70 transecting across Europe, to northwest Africa and into eastern North America. The final stages

71 of Pangea amalgamation (e.g. Nance et al., 2010) modified the Western Europe sector of the
72 belt into its characteristic sinuous shape. Today, this tectonic belt traces at least one, and
73 perhaps four arcs from Poland to Brittany, and then across the Bay of Biscay (Cantabrian Sea)
74 into Iberia, where the system is truncated by the younger Betic Alpine orogeny in southeast
75 Iberia (Fig. 1; e.g. Weil et al., 2013). The southern truncation of the Variscan in Europe hinders
76 a precise correlation with equivalent age outcrops in NW Africa.

77 Within the Iberian Peninsula, the orogen is characterized by two large-scale curves (Fig.
78 2): (1) to the north is the well-studied and nearly 180° secondary orocline, the Cantabrian (a.k.a.
79 Ibero-Armorican) Orocline, which buckled a segment of the Variscan belt from ~315 to ~290 Ma
80 (e.g. Weil et al., 2019 and references therein); and (2) to the south is a curve with disputed
81 magnitude and kinematics that is usually referred to as the Central Iberian curve/orocline or
82 Castillian bend (Martínez-Catalán et al., 2015). Though there remains tremendous uncertainty
83 on the geometry and kinematics of the Central Iberian curve, multiple hypotheses exist as to its
84 nature, and disagreements continue on its importance in the tectonic evolution of Europe during
85 the waning stages of Paleozoic global supercontinent construction. The diversity of
86 interpretations on the Central Iberian curve range from a nonexistent structure (Dias et al.,
87 2016), to being one of the most important pieces in our understanding of the late Carboniferous
88 and Permian geodynamics of the Iberian Variscan system (e.g. Martínez-Catalán et al., 2011;
89 2014).

90 This paper reviews the most recent advances on the geometry and kinematics of the
91 Central Iberian curve, synthesizing what we know and what we don't, and ending with a
92 discussion of the main unsolved issues. We hope that this paper fosters novel studies that will
93 lead to a better understanding of when and which mechanisms acted in the aftermath of the
94 Variscan-Alleghanian orogeny.

95 **2 The long and winding orogen**

96 The Variscan (Europe-NW Africa)-Alleghanian (North America) orogeny is a continental-
97 scale tectonic system (1000 km wide and >8000 km long) that sutured Gondwana and
98 Laurussia together, forming the supercontinent Pangea (e.g. Domeier and Torsvik, 2014; Edel
99 et al., 2018; Pastor-Galán et al., 2019a). The fragments of this system are now dispersed over
100 three continents, Europe, Africa and North America due to the Mesozoic break-up of Pangea
101 (Buitter and Torsvik, 2014; Keppie, 2015). This orogen formed as a consequence of a long and
102 protracted tectonic history that involved several events, from initial convergence (ca. 420 Ma;
103 e.g. Franke et al., 2017), to the consumption of multiple putative oceanic tracts and/or basins

104 that existed between Gondwana and Laurussia (ca. 280 Ma; e.g. Kirsch et al., 2012). The
105 Variscan-Alleghanian orogen itself represents the closing of at least one major ocean, the Rheic
106 (e.g. Nance et al., 2010), whose axial ridge likely failed or subducted at ca. 395 Ma along its
107 paleo-northern margin (e.g. Woodcock et al., 2007; Gutiérrez-Alonso et al., 2008a). Perhaps the
108 orogeny involved other large oceans (Stampfli and Borel, 2002; Franke et al., 2017; 2019), but
109 most surely involved several minor seaways and basins that existed between Gondwana,
110 Laurussia, and several intervening micro-continents (e.g. Azor et al., 2008, Dallmeyer et al.,
111 1997; Kroner and Romer, 2013; Díez-Fernández et al., 2016; Pérez-Cáceres et al., 2017). The
112 final continent-continent collision began after closure of all oceans and intervening seaways.
113 The commencement of this deformation was diachronistic and became progressively younger
114 westwards (in present-day coordinates): with Devonian continent-continent collisions along the
115 eastern boundary, progressing to earliest Permian ages in the westernmost sector (McWilliams
116 et al., 2013; Chopin et al., 2014; López-Carmona et al., 2014; Franke et al., 2017).

117 The present-day geometry of the Variscan-Alleghanian systems has a contorted trace
118 (Fig. 1). In Europe, from east to west, the trend starts with a prominent curve around the
119 Bohemian massif (e.g. Tait et al., 1996), followed by a deflection in the Ardennes-Bravant (e.g.
120 Zegers et al., 2003). In Brittany the outer curvature of the Cantabrian or Ibero-Armorican
121 orocline begins (e.g. van der Voo et al., 1997), and wraps nearly 180° around and across the
122 Bay of Biscay as it turns in NW Iberia. The Central Iberian curve marks the final concave to the
123 west curve (in present-day coordinates) and is the focus of this paper (e.g. Aerden, 2004;
124 Martínez Catalán, 2011; Shaw et al., 2012). The orogen continues in North America where, from
125 north to south, it has salients and recesses that undulate back and forth from Atlantic Maritime
126 Canada (e.g. O'Brien, 2012) down along the Pennsylvanian and into the Alabama curves (e.g.
127 Thomas, 1977).

128 Interpretation on the origin of these curvatures varies widely. The curvatures in North
129 America are argued to be the result of a preexisting irregular margin of Laurentia due to the
130 break-up of the Rodinia supercontinent, which resulted in the formation of orogenic salients and
131 recesses during subsequent Appalachian collision (e.g. Rankin, 1976; Thomas, 1977, 2004). In
132 this case, vertical-axis rotations affected mainly the upper crustal levels during orogenesis (e.g.
133 Marshak, 1988; Bayona et al., 2003; Hnat and van der Pluijm, 2011). In Europe, the Bohemian
134 and Ardennes-Bravant massif curvatures have poor kinematic constraints. In the Bohemian
135 Massif, some suggest secondary rotations formed an orocline (Tait et al., 1996), while others
136 suggest little to no vertical-axis rotations and a primary arc (Chopin et al., 2012). The Ardennes-
137 Bravant Massif recorded some vertical-axis-rotations (e.g. Molina-Garza and Zeijderveld, 1996),

138 but it is unclear if these are a response to progressive or secondary oroclinal bending, or
139 whether rotations only affected the upper crust. The most outstanding example of Variscan-
140 Alleghanian orogen curvature is exposed in the Iberian Massif, with the Cantabrian Orocline and
141 the coupled curvature of Central Iberia.

142 2.1 Two of us: The Variscan orogen in Iberia

143 The western half of the Iberian Peninsula constitutes the Iberian massif, one of the
144 largest exposures of the Variscan orogen and the only place that contains an almost continuous
145 cross section of the orogen (Fig. 2; e.g. Lotze 1945, Julivert 1974, Pérez-Estaún et al., 1991;
146 Ayarza et al., 1998; Simancas et al., 2003; Ribeiro et al. 2007, Martínez Catalán et al., 2014,
147 2019). The majority of the Iberian Massif contains Gondwanan affinity rocks (e.g. Murphy et al.,
148 2008; Pastor-Galán et al., 2013a; Gutiérrez-Marco et al., 2017) and likely represents a proximal
149 piece of the Gondwana margin until its final amalgamation with Pangea (e.g. Pastor-Galán et
150 al., 2013b). Owing to the stratigraphic, structural and petrological styles, the Iberian Massif has
151 been traditionally divided into six tectonostratigraphic zones (Fig. 2; Lozte, 1945; Julivert, 1971):
152 (1) The Cantabrian Zone represents a Gondwanan thin-skinned foreland fold-and-thrust belt. It
153 has overall low-grade internal deformation and metamorphism, and represents shortening that
154 occurred during Mississippian times (e.g. Marcos and Pulgar, 1982; Pérez Estaún et al., 1988;
155 Gutiérrez-Alonso 1996; Alonso et al., 2009; Pastor-Galán et al., 2009; 2013b). (2) The West-
156 Asturian Leonese Zone represents a metamorphic fold-and-thrust belt with Barrovian
157 metamorphism that collapsed coevally with thrust emplacement onto the Cantabrian Zone (e.g.
158 Martínez-Catalán et al., 1992; Alcock et al., 2009; Martínez-Catalán et al., 2014). (3) The
159 Central Iberian Zone represents the Gondwanan hinterland with Barrovian and Buchan
160 metamorphism and is intruded by igneous rocks of various ages (e.g. Macaya et al., 1991; Díez
161 Balda, 1995; Gutiérrez-Alonso et al., 2018). (4) The Ossa-Morena Zone represents the most
162 distal zone of the Gondwana platform, and is characterized by a metamorphic fold-and-thrust
163 belt with dominantly sinistral displacement (e.g. Robardet and Gutiérrez-Marco, 2004; Quesada,
164 2006). (5) The Galicia-Tras-os-Montes Zone represents a far-travelled allochthonous terrane
165 that contains high-pressure units and relicts of oceanic-like crust (e.g. López-Carmona et al.,
166 2014; Martínez-Catalán et al., 2019). (6) The South Portuguese Zone represents a foreland
167 fold-and-thrust belt with little internal deformation and metamorphism with Avalonian affinity and
168 a strong sinistral component of shear (e.g. Pereira et al., 2012; Pérez-Cáceres et al., 2016;
169 Oliveira et al., 2019). Geographically, the external zones of the Gondwana margin are nested to
170 the north into the core of the Cantabrian Orocline, whereas the hinterland zones are to the west

171 and center of the massif (Fig. 2; e.g. Díaz Balda, 1995; Azor et al., 2019). The southwestern-
172 most extent of Iberia contains a putative suture of the Rheic Ocean, as well as a piece of the
173 Laurussian margin fold-and thrust belt, today preserved in the South Portuguese Zone (e.g.
174 Pereira et al., 2012, 2017; Oliveira et al., 2019).

175 The Gondwanan autochthon stratigraphy (Cantabrian, West Asturian-Leonese, Central
176 Iberian and Ossa Morena zones) consist of a Neoproterozoic arc and back-arc basin (e.g.
177 Fernández-Suárez et al., 2014), which evolved to a rift-to-drift Cambrian to Early Ordovician
178 sequence and then to an Ordovician to Late Devonian passive margin basin sequence (e.g.
179 Sánchez-García et al., 2019; Gutiérrez-Marco et al., 2019; Gutiérrez-Alonso et al., in press).
180 Overall the system transitioned from a relatively isolated Early Cambrian continental basin, to a
181 restricted marine basin, to development of an open marine platform that was locally punctuated
182 by magmatism (e.g. Gutiérrez-Alonso et al., 2008b; Palero-Fernández, 2015). The Ossa
183 Morena Zone represents the outermost platform, followed by an intermediate platform
184 characterized by an asymmetric horst (Central Iberian Zone) and graben (West-Asturian
185 Leonese Zone), which ends in the innermost shelf environment of the Cantabrian Zone (Fig. 3;
186 e.g. Gutiérrez-Marco et al., 2019). The differences between the West Asturian-Leonese and
187 Central Iberian Zone are mainly deeper vs. shallower sedimentary facies (respectively) and a
188 local Lower Ordovician unconformity in the Central Iberian Zone (Toledanian, e.g. Álvaro et al.,
189 2018), which places Lower Ordovician strata atop pre-Cambrian to Cambrian rocks (Fig. 3; e.g.
190 Gutiérrez-Marco et al., 2019). The Central Iberian Zone is divided into two domains: (1) The Ollo
191 de Sapo domain, which contains abundant Lower Ordovician magmatism of calc-alkaline affinity
192 (e.g. Díez Montes, 2006; Gutiérrez-Marco et al., 2019); and (2) the 'Schistose–Greywacke
193 domain' characterized by a predominance of outcrops of Neoproterozoic to Lower Cambrian
194 sedimentary rocks (e.g. Gutiérrez-Marco et al., 2019 and references therein).

195 The Galicia Tras-os-Montes Zone (Farias et al., 1987) is a complex structural stack
196 including a basal schistose unit (Parautochthon; Dias da Silva et al., 2020) structurally overlain
197 by mafic rocks with an oceanic-like signature and other allochthonous rocks under high-
198 pressure metamorphism (e.g. López-Carmona et al., 2014; Martínez-Catalán et al., 2019). The
199 oceanic rocks of this zone are classically interpreted as a Rheic Ocean suture (e.g. Martínez
200 Catalán et al., 2009). Recent interpretations support its origin as a minor oceanic basin or
201 seaway within the realm of Gondwana (e.g. Pin et al., 2002; Arenas et al., 2016).

202 The South Portuguese Zone constitutes the Laurussian foreland fold-and-thrust belt in
203 the Iberian Variscides (e.g. Pereira et al., 2012; Pérez-Cáceres et al., 2017). It contains three
204 units: (1) the Pulo de Lobo, a low grade metamorphic accretionary prism with clastic

205 sedimentary rocks and basalts with MORB signature (e.g. Azor et al., 2019; Pérez-Cáceres et
206 al., this volume) sometimes considered an independent zone; (2) The Iberian Pyrite Belt, which
207 is a world class volcanogenic massive sulfide deposit formed between 390 and 330 Ma (e.g.
208 Oliveira et al., 2019a; 2019b); and (3) the Baixo Alentejo Flysch, which is located to the
209 southwest and is a syn-orogenic composite turbiditic sequence with ages from ~330 to ~310 Ma
210 (Oliveira et al., 2019b). The boundary between the South Portuguese and Ossa Morena zones
211 is a sinistral shear zone (the so-called Southern Iberian shear zone in the Beja-Acebuches
212 oceanic-like unit, Crespo-Blanc and Orozco, 1988; Quesada and Dallmeyer., 1994; Pérez-
213 Cáceres et al., 2016) that contains a strongly deformed amphibolitic belt with oceanic affinity
214 (Munha et al., 1986; Munha, 1989; Quesada et al., 2019). This belt potentially represents
215 dismembered relics of the Rheic Ocean and/or a subsidiary seaway that opened during a
216 Variscan transtension event in SW Iberia (e.g. Pérez-Cáceres et al., 2015; Quesada et al.,
217 2019).

218 Finally, Paleozoic rocks occur sporadically within the Alpine Betic chain. Their lithological
219 monotony, paucity of fossils, and the intensity of deformation and metamorphism during Alpine
220 orogeny, make recognizing the original features of the different successions challenging (e.g.
221 Martín-Algarra et al., 2019). Some faunal and detrital zircon studies suggest that the Paleozoic
222 outcrops in the Betics may be similar to the most continentalward realms of the Gondwanan
223 platform (i.e., the Cantabrian Zone; e.g. Rodríguez-Cañero et al., 2018; Jabaloy-Sánchez et al.,
224 2018). Following the latest plate reconstructions of the Mediterranean during Meso-Cenozoic
225 times, the Paleozoic units of the Betic-Rif chain may have been located proximal to the present-
226 day position of the Balearic Islands (van Hinsbergen et al., 2020).

227 The Variscan orogen in Iberia shows multiple deformation, metamorphic, and magmatic
228 events (e.g. Martínez-Catalán et al., 2014; Azor et al., 2019; Fig. 2) that evolved diachronously
229 from the suture towards the external zones (Dallmeyer et al., 1997): (1) An initial continent-
230 continent collision began ca. 370-365 Ma, which produced high-pressure metamorphism (e.g.
231 Lopez-Carmona et al. 2014). (2) Between 360 and 330 Ma a protracted shortening phase
232 occurred, frequently divided into main phases C1 and C2, that were accompanied by Barrovian
233 type metamorphism (e.g. Dias da Silva et al., 2020) and plutonism at ~340 Ma (e.g. Gutiérrez-
234 Alonso et al., 2018). (3) An extensional collapse event, so-called E1, occurred at ~333-317 Ma,
235 which formed core-complexes and granitic domes in the Central Iberian and West Asturian-
236 Leonese zones (Fig. 2C; e.g. Alcock et al., 2009; Díez-Fernández and Pereira, 2016; López-
237 Moro et al., 2018). This event is coeval and genetically linked to the formation of the foreland
238 fold-and-thrust-belt of the Cantabrian Zone (e.g. Gutiérrez-Alonso, 1996). (4) A late

239 Carboniferous shortening event (C3) occurred ca. 315-290 Ma and is interpreted to have
240 resulted in the formation of the Cantabrian Orocline and was accompanied by intrusion of
241 mantle derived granitoids (Fig. 2C; e.g. Gutiérrez-Alonso et al., 2011a, 2011b; Pastor-Galán et
242 al., 2012a). (5) A final early Permian extensional event (E2), mostly found in the Central Iberian
243 Zone, resulted in the formation of core complexes and regional doming (Dias da Silva et al.,
244 2020). (6) A final shortening event (C4), possibly coeval with E2, resulted in widespread brittle
245 deformation (e.g. Azor et al., 2019; Fernández-Lozano et al., 2019).

246 In SW Iberia, the aforementioned Variscan deformation events are characterized by a
247 dominant sinistral component, which contrasts with the general dextral component recognized in
248 most other regions of the orogen (e.g. Martínez Catalán et al., 2011; Gutiérrez-Alonso et al.,
249 2015). Early collisional structures (C1) formed NE-vergent recumbent folds in the southernmost
250 Central Iberian Zone and SW-vergent folds and thrusts in the Ossa Morena and South
251 Portuguese zones. This phase continued with a transtensional event that heterogeneously
252 extended the continental lithosphere (e.g. Pérez-Cáceres et al. 2015). Coevally, an important
253 extension-related magmatic event happened, perhaps assisted by a plume-type mantle
254 (Simancas et al. 2006) or because of slab break-off (Pin et al. 2008). After this transtensional
255 event, significant sinistral transpression occurred forming the extensive shear zones to the north
256 and south of the Ossa Morena Zone (Fig. 2B), which accommodated the majority of transcurrent
257 motion. However, sinistral displacements are observed all along the Ossa Morena and South
258 Portuguese zones. Pérez-Cáceres et al. (2016) estimated over 1000 km of collisional
259 convergence in SW Iberia, most of which corresponds with sinistral displacements parallel to
260 terrane boundaries.

261 3 Synthesis on the Geometry and Kinematics of the Cantabrian 262 Orocline

263 Understanding the geometry, kinematic evolution and mechanics of curved mountain
264 systems is crucial to developing paleogeographic and tectonic reconstructions and
265 understanding past geodynamics (e.g. Marshak, 2004; Van der Voo, 2004; Li et al., 2012; van
266 Hinsbergen et al., 2020). Introduced by Carey (1955 p.257), an orocline (from Greek ορος,
267 mountain, and κλινο, bend) is "...an orogenic system, which has been flexed in plan to a horse-
268 shoe or elbow shape." Although sometimes used in the literature as a geometric description of
269 any orogenic curvature, herein orocline is strictly used as a the term for map-scale bends that
270 underwent vertical-axis rotations (Weil and Sussman, 2004; Johnston et al., 2013; Pastor-Galán
271 et al., 2017a). The kinematic classification of curved mountain belts (Weil and Susman, 2004;

272 Johnston et al, 2013) distinguishes two end members: (1) Primary orogenic curves, which
273 describe those systems in which curvature is a primary feature of the orogen and formed
274 without significant or systematic vertical-axis rotations, and (2) Secondary oroclines, where
275 orogenic curvature was acquired due to vertical-axis rotations subsequent to primary orogenic
276 building. Those systems whose curvature is the product of vertical-axis rotation during the
277 primary orogenic pulse and/or only a portion of the observed curvature is secondary are termed
278 progressive oroclines.

279 The orocline test (or strike test), evaluates the relationship between changes in regional
280 structural trend (relative to a reference trend for an orogen) and the orientations of a given
281 geologic fabric element or magnetization (relative to a reference direction). In terms of
282 evaluating developmental kinematics, the most relevant geologic marker is paleomagnetic
283 declination, which can be used to quantitatively evaluate total and systematic rotations as a
284 function of along-strike variability. Once acquired, data is plotted on Cartesian coordinate axes
285 with the strike (S) of the orogen (relative to a reference) along the horizontal axis, and the fabric
286 azimuth (F, relative to a reference) along the vertical axis. The test originally used a basic least-
287 squares (OLS) regression (Schwartz and Van der Voo, 1983) to estimate the slope (coded m in
288 formulas), ideally between 0 and 1, which then is interpreted with respect to vertical-axis
289 kinematics. More recently, Yonkee and Weil (2010b) and Pastor-Galán et al. (2017a) introduced
290 more robust statistics to estimate the correlations slope and its uncertainty, considering and
291 propagating errors of the input data. Primary orogenic bends show no change of paleomagnetic
292 declination orientations with varying structural trend, and therefore the slope is expected to be 0.
293 In progressive oroclines, the declination variation records some fraction of the total observed
294 orogenic strike variability, and thus the slope would range between 0 and 1, depending on the
295 amount of primary curvature. Secondary oroclines are those in which the paleomagnetic vectors
296 record 100% of the rotation, yielding slopes of 1, meaning that the orogenic system must have
297 started as a roughly linear system that then underwent secondary vertical-axis rotations until its
298 present-day curvature was acquired. The slope obtained with the orocline test can only be
299 confidently interpreted when the chronology of fabric formation is well known.

300 The trend of the Variscan belt in Iberia follows a sinuous “S” shape that is especially
301 prominent in the northwest region of the Iberian Peninsula, and then becomes more subtle due
302 to the predominance of younger cover sequences in the central and eastern regions of the
303 peninsula (Fig. 1 and 2). This dramatic geometry has stimulated a century long scientific debate
304 as to its origin (e.g. Suess, 1892; Staub, 1926; Martínez Catalán et al., 2015). To the north and
305 convex to the west is the Cantabrian Orocline, and to the center-south and convex to the east is

306 the Central Iberian curve. The overall trend of the Cantabrian Orocline starts in Brittany (France)
307 and southern England and then curves through the Bay of Biscay and then south into central
308 north Iberia (Fig. 1, 2 and 4). The Cantabrian Orocline (also known as Ibero-Armorican Orocline/
309 Arc, Asturian Arc or Cantabrian-Asturias Arc) is arguably the first curved orogen that was
310 scientifically described, recognized by the change in structural trend of mapped thrusts and fold
311 axes (Schultz, 1858, Barrois, 1882, Suess, 1892). The Cantabrian Orocline traces an arc with a
312 curvature close to 180° within the central Cantabrian Zone (the Gondwanan foreland in Iberia,
313 fig. 2), and opens to approximately 150° as one moves to the outer arc reaches (Fig. 1). At the
314 crustal-scale, the Cantabrian Orocline represents a first-order vertical-axis buckle fold in plan-
315 view that refolds pre-existing Variscan structures (e.g. Julivert and Marcos, 1973; Weil et al.,
316 2001). The inner arc of the orocline, or the Cantabrian Zone is characterized by tectonic
317 transport towards the core of the orocline, i.e., the orocline has a contractional core, where low
318 finite strain values and locally developed cleavage occur (Pérez-Estaún et al., 1988; Gutiérrez-
319 Alonso, 1996; Pastor-Galán et al., 2009). Within the inner core a variety of structures record
320 non-coaxial strain, which produced complex interference folds and rotated thrust sheets (e.g.
321 Julivert and Marcos, 1973; Julivert and Arboleya, 1984; Pérez-Estaún et al, 1988; Aller and
322 Gallastegui, 1995; Weil, 2006, 2013; Pastor-Galán et al., 2012b; Shaw et al., 2015; 2016a; Del
323 Greco et al., 2016). In contrast, the outer arc shows a vertical-axis fold with a ca. 150° interlimb
324 angle that was accommodated by significant shearing, both dextral and, in lesser amounts,
325 sinistral that was penecontemporaneous to vertical-axis rotation (Gutiérrez-Alonso et al., 2015).
326 Weil et al. (2013, 2019) extensively review the geometry of the Cantabrian Orocline.

327 All kinematic data studied so far support a model in which the Cantabrian Orocline
328 formed due to secondary vertical-axis rotation in a period of time younger than 315 Ma and
329 older than 290 Ma. Overall, the southern limb of the orocline rotated counterclockwise (CCW)
330 and the northern limb clockwise (CW; Fig. 4). Orocline formation happened subsequent to the
331 main shortening phases of the orogen (C1 and C2) and late-stage orogenic collapse (E1), and
332 therefore, it is an ideal example of a secondary orocline in the strictest sense. Development of
333 the Cantabrian Orocline requires the existence of a roughly linear orogenic belt during early
334 Variscan closure of the Rheic Ocean (with a roughly N-S orientation in present-day
335 coordinates), which was subsequently bent in plan-view into an orocline during late stages of
336 Pangea amalgamation. Such interpretation is grounded in extensive paleomagnetic (e.g. Hirt et
337 al., 1992; Parés et al. 1994; Stewart, 1995; van de Voo et al., 1997; Weil, 2006; Weil et al.,
338 2000; 2001; 2010), along with important contributions from structural (e.g. Gutiérrez-Alonso
339 1992; Kollmeier et al., 2000; Merino-Tomé et al., 2009; Pastor-Galán et al., 2011; 2014; Shaw et

340 al., 2015) and geochronological studies (e.g., Tohver et al., 2008; Gutiérrez-Alonso et al., 2015).
341 Weil et al. (2013) provided a comprehensive review on the kinematic constraints, updated in
342 2017a by Pastor-Galán et al., and in 2019 by Weil et al.

343 4 The intriguing geometry of the Central Iberian curve

344 The more southern Central Iberian curve has a similar magnitude, but opposite
345 curvature compared to the Cantabrian Orocline (Fig. 1 and 2B). This structure has been referred
346 to as the Central Iberian curve, arc, bend or orocline. In this paper we use 'Central Iberian
347 curve'. The other aforementioned terms involve still unknown parameters or are misleading:
348 e.g., orocline implies kinematics (Weil and Sussman, 2004); bend refers to a mechanism of
349 formation (e.g. Fossen, 2016); and arc could be ambiguous, since the term is commonly used
350 for volcanic chains. The Central Iberian curve was first described by Staub (1926) and was
351 termed the Castilian bend. Continental drift pioneers paid some attention to Staub's description
352 (e.g. Holmes, 1929; Du Toit, 1937), but the curved structure remained largely ignored for
353 multiple decades (e.g. Martínez Catalán et al., 2015). The hypothesis of a large-scale curvature
354 in Central Iberia made a comeback at the beginning of the 21st century with a study of Variscan
355 porphyroblast kinematics across Iberia by Aerden (2004). Since then, several attempts to unveil
356 its geometry and kinematics have given contrasting results.

357 The elusive nature of the Central Iberian curve resides in the poor exposure of its
358 putative hinge (Fig. 2). The hinge of the Cantabrian orocline crops out extensively and the
359 changes in thrust and fold axes trend are observable at high-resolution from aerial photographs
360 and are readily mapped using outcrop-scale observations. In contrast, the alleged hinge of the
361 Central Iberian curve is largely covered by Mesozoic and Cenozoic basins (Fig. 2). The
362 curvature is most recognizable at the boundary between the Galicia-Tras os Montes and Central
363 Iberian zones (Fig. 2A; Aerden, 2004; Martínez Catalán, 2012). The thrust fault that bounds
364 those areas traces close to a 180° of curvature and marks the emplacement of the most distal
365 units. Before the revival of Staub's curved geometry along the entire Central Iberian Zone, there
366 were several attempts to explain the curved shape of the Galicia Tras-os-Montes Zone. Some
367 consider the Galicia Tras-os-Montes Zone a block that escaped during an early Variscan (C1)
368 non-cylindrical collision, forming a extrusion wedge towards areas that underwent lesser amount
369 of shortening (Martínez-Catalán, 1990, Dias da Silva et al., 2015; 2020); or alternatively a klippe
370 of a larger allochthonous thrust sheet, or the product of an interference pattern between C2, E1
371 and C3 structures (e.g. Ries and Shackleton, 1971; Martínez Catalán et al., 2002; Rubio
372 Pascual et al., 2013; Díez-Fernández et al., 2015).

373 In addition to the Galicia Tras-os-Montes Zone, the other areas that show a certain
374 degree of curvature are to the E and SE of the Central Iberian Zone. There, an approximately
375 20° change in strike of the Iberian ranges (NE Iberia, Fig. 2A) is observed, which represents the
376 only known outcrop of the hinge of the Central Iberian curve's outer arc. The rest of the
377 curvature has been implied with indirect observations leading to three competing geometric
378 proposals for the Central Iberian curve (Fig. 2B). The main arguments used to constrain the
379 geometry of the Central Iberian curve are: (1) the geometry of Galicia Tras-os-Montes folds and
380 the orientation of observed garnet inclusion trails (Aerden, 2004; Fig. 2B-1); (2) the alignment of
381 aeromagnetic anomalies and fold trends in the Iberian ranges and the E-SE Central Iberian
382 Zone (Martínez-Catalán, 2012; Fig. 2A and 2B-2) and; (3) the regional distribution of
383 paleocurrents recorded in Ordovician quartzites (Shaw et al., 2012; Fig. 2B-3 and 3). All
384 proposed geometries share two features: (1) The curvature runs parallel to the Central Iberian
385 Zone, and is located in the center-west of Iberia, and (2) all place the Galicia Tras-os-Montes
386 Zone in the core of the curve with the curved axial traces cross-cutting the Morais Complex,
387 which is a set of mafic and ultramafic rocks that is roughly circular in shape (Fig. 2B; Dias da
388 Silva et al., 2020).

389 Aerden (2004) compared the orientation of inclusions in metamorphic porphyroblasts
390 across the Variscan allochthonous terranes of the NW Iberian Massif, and found that inclusion
391 trails maintain a constant north–south orientation. Comparing such results with the trend of the
392 Variscan fold axes in the Central Iberian Zone (Fig. 2A) and a novel interpretation of the
393 aeromagnetic anomalies of the Iberian Peninsula (Fig. 5A), Aerden suggested a geometry in
394 which the Central Iberian curve was more prominent in the outer arc than in the inner arc (Fig.
395 2B-1). In Aerden's view the geometry of the Galicia Tras-os Montes Zone does not represent a
396 large-scale curvature, but rather the original shape of the nappe, perhaps re-tightened during
397 C3 deformation. In contrast, the Iberian Ranges and the SE Central Iberian Zone represent the
398 more curved sector (Fig. 2B-1). In the model of Aerden (2004), the Ossa Morena and South
399 Portuguese zones are not part of the Central Iberian curvature.

400 Martínez-Catalán (2012) reinterpreted Aerden's analysis of aeromagnetic map data (Fig.
401 5A) and their interpreted structural trends of C1-C2 fold axes from Central Iberian Zone
402 structures (Fig. 2A). In Martínez-Catalán's model, the Central Iberian curvature is a symmetric
403 arcuate shape in which orogen trend changes equally in the inner and outer arc, and is
404 comparable in size to the Cantabrian Orocline, but with opposite curvature and less shortening.
405 This geometric model also excludes the Ossa Morena and the South Portuguese Zones as
406 elements involved in the formation of the curvature (Fig. 2B-2).

407 Finally, Shaw et al. (2012) studied the orientation of paleocurrents in Ordovician
408 Armorican Quartzite (e.g. Aramburu, 2002), which is one of the most prominent rocks exposed
409 in Iberia (Fig. 3). These authors found that paleocurrents fanned outward with respect to the
410 Cantabrian Orocline curve and are approximately perpendicular to the structural trend
411 throughout the peninsula (Fig. 3). Shaw et al. (2012) assumed that the direction and sense of
412 paleocurrents were originally parallel throughout all zones, and concluded that the Central Iberia
413 curve is part of a 'S' shape isoclinal structure with a similar magnitude of curvature to the
414 Cantabrian Orocline (Fig. 2B-3). It is unclear from the Shaw et al. (2012) model what the
415 involvement of the Ossa Morena and South Portuguese zones in the overall curve is (if any),
416 nor the prospective location of the external zones of the orogen (Cantabrian Zone) with respect
417 to the overall curvature.

418 5 Move over once, move over twice: Kinematic constraints

419 Late Variscan kinematic data (315-290 Ma; C3, E2, C4 phases) in the Central Iberian
420 curve were scarce prior to revival of Staub's Central Iberian curve (e.g. Vergés, 1983; Julivert et
421 al., 1983; Parés and van der Voo, 1992). More recently, a wealth of studies have been
422 published on the kinematics of forming the Central Iberian curve (Fig. 2B), which are reviewed
423 below.

424 5.1 Structural Geology and Geochronology

425 Curved orogens that result from differential vertical-axis rotations develop remarkable
426 structures within their hinges where compressive and extensive radial structures often develop
427 in combination with tangential shear structures (e.g. Li et al., 2012; Eichelberger and McQuarrie,
428 2015). With the re-emergence of the Central Iberian curve debate, several studies have re-
429 evaluated the well-documented structures from the Central Iberian Zone to constrain the origin
430 and kinematics of curvature. The majority of studies focused on the hinge zone of the curve in
431 the area surrounding Galicia Tras-os-Montes (e.g. Dias da Silva et al., 2014; Jacques et al.,
432 2018a), but some do explore areas in the outer-arc (e.g. Palero-Fernández et al., 2015;
433 Gutiérrez-Alonso et al., 2015). The following section synthesizes the findings of new field,
434 structural, and geochronological analyses from around the hinge of the Central Iberian curve
435 and its surrounding regions. The reviewed studies identify several deformation events that are
436 linked to regional Variscan deformation phases (Fig. 2A).

- 437 1. An early generation of upright to overturned cylindrical folds with an associated axial
438 planar cleavage (C1). The C1 fold axes plunge variably from horizontal to nearly vertical

439 (e.g. Jacques et al., 2018a, 2018b). The original trend of the fold axes were parallel to
440 the orogen (e.g. Pastor-Galán et al., 2019b), however interference with younger
441 deformation events has created complicated geometries (e.g. Díez Fernández et al.,
442 2013; Palero-Fernández et al., 2015). The emplacement of the allochthonous units of
443 the Galicia Tras-os-Montes Zone (commonly referred as C2) is closely associated with
444 development of C1 folds, but is restricted to shear zones located along the boundary
445 between the latter and the Central Iberian Zone (Dias da Silva et al., 2020). This phase
446 includes orogen-parallel emplacement of the allochthonous Galicia Tras-Os Montes
447 units and its associated thrusts (Fig. 2A). The non-coaxial nature of the emplacement of
448 this allochthonous nappe produced folding interference and local vertical-axis rotations
449 (Dias da Silva et al., 2020). Prograde Barrovian metamorphism (known as M1) reached
450 its pressure peak at the end of C2 (Rubio Pascual et al., 2013).

451 2. After C1 and C2, the resulting thickened crust gravitationally collapsed (Macaya et al.,
452 1991; Escuder Viruete et al., 1994; Díaz-Balda et al., 1995; Díez-Montes, 2010). This
453 gravitational collapse (phase E1) formed gneiss-dome core complexes between 330 and
454 317 Ma (e.g. Díez Fernández and Pereira, 2016) especially in the core of the Central
455 Iberian curve (Fig. 2C; e.g. Martínez-Catalán, 2012). This phase formed large
456 subhorizontal extensional detachments that exhumed to depths of the middle crust (e.g.
457 Rubio-Pascual et al., 2013; Dias da Silva et al., 2020). General decompression
458 produced a Buchan-type metamorphic event (M2; e.g. Rubio-Pascual et al., 2016, Solís-
459 Alulima et al., 2019) and widespread anatexis melting (e.g. López-Moro et al., 2018;
460 Pereira et al., 2018). The E1 phase developed a fold system with sub-horizontal axes
461 and a penetrative subhorizontal cleavage (e.g. Dias da Silva et al., 2020). Mapped
462 folding geometries indicate the deflection of C1 folds into overturned positions within the
463 E1 deformation zones (e.g. Díez Fernández et al., 2013; Díez Fernández and Pereira,
464 2016; Pastor-Galán et al., 2019b). In addition to large-scale extensional deformation and
465 Buchan metamorphism, E1 developed a regional dome-and-basin pattern, resulting in
466 portions of the allochthonous terranes tectonically transported into basins (e.g. Días da
467 Silva et al., 2020).

468 3. The structures developed during C1-C2 compression and E1 extension, are re-folded by
469 a younger shortening phase (C3; syn-Cantabrian Orocline). C3 formed upright open
470 folds and conjugate sub-vertical shear zones (e.g. Gutiérrez-Alonso et al., 2015; Díez
471 Fernández and Pereira, 2017; Dias da Silva et al., 2020). C3 was coeval with regional
472 retrograde metamorphism (M3) and with intrusion of mantle derived granitoids (Fig. 2C;

473 e.g. Gutiérrez-Alonso et al., 2011a), surrounded by contact metamorphic aureoles (e.g.
474 Yenes et al., 1999). The age of the C3 event ranges from 315 and 290 (e.g. Jacques et
475 al., 2018a), and is concomitant with the formation of the Cantabrian Orocline (e.g.
476 Pastor-Galán et al., 2015a). Ductile deformation, including folding with axial planar
477 cleavage (e.g. Dias da Silva et al., 2020; Pastor-Galán et al., 2019b) and the
478 development of conjugate shear zones, occurred at the early stages of C3 (315-305 Ma;
479 Gutiérrez-Alonso et al., 2015; Díez-Fernández and Pereira, 2017; Jacques et al., 2018b)
480 and was followed by brittle deformation that formed cross-joint sets and vein swarms
481 with Sn-W mineralizations (Jacques et al., 2018a; 2018b). The conjugated shear zones,
482 some of them with hundreds of kilometers of displacement, had activity during the period
483 315-305 Ma based on direct Ar-Ar dating of the shear zones (Gutiérrez-Alonso et al.,
484 2015) and cross-cutting relationships with precisely dated igneous rocks (Díez-
485 Fernández and Pereira, 2017). Note that these shear zones show a younger age with
486 respect to the sinistral shear zones that bound the Ossa Morena and South Portuguese
487 zones (340-330 Ma; e.g. Dallmeyer et al., 1993). New studies in the Central Iberian
488 Zone have determined that several folds, previously interpreted as C1 (e.g. the
489 Tamames-Marofa-Sátão synform) are in fact C3 structures, possibly nucleated within
490 existing C1-C2 structures (e.g. Dias da Silva et al., 2017; Jacques et al., 2018b). The
491 remarkable continuity along the Central Iberian Zone of these folds (Fig. 2A), previously
492 interpreted as C1 (e.g. Díez-Balda et al., 1990; Abalos et al., 2002; Dias and Ribeiro,
493 1994; Dias et al., 2016), suggests the ubiquity and importance of this deformation phase.

494 4. The N-S shortening (in present day coordinates) of C3 deformation continued through
495 the Early Permian under brittle conditions (so-called C4 event) (e.g. Dias da Silva et al.,
496 2020) and overlapped with the formation of E2 extensional faults (Fig. 2A; Dias and
497 Ribeiro 1991; Dias et al. 2003; Rubio Pascual et al., 2013; Arango et al., 2013;
498 Fernández-Lozano et al. 2019; Dias da Silva et al., 2020). C4 N-S compression
499 produced a series of NNE-SSW and NNW-SSE brittle faults (Gil Toja et al. 1985; Dias
500 and Ribeiro 1991; Dias et al. 2003; Fernández-Lozano et al., 2019) and associated sub-
501 vertical and sub-horizontal widespread kink-bands (e.g. Aller et al., 2020; Dias da Silva
502 et al., 2020) that are today exposed in Northern Iberia. E2 developed core complex-like
503 structures with extensional shear zones that further telescoped M2 metamorphic
504 isograds between the anatectic cores of gneiss domes and the associated hanging wall
505 units. This event favored sub-horizontal folding, and crenulation cleavage development
506 in the footwall together with kink-band generation in the upper low-grade structural

507 levels.

508 5.2 Paleomagnetism

509 Paleomagnetism investigates the Earth's ancient magnetic field as it is recorded in
510 rocks. Among other features, rocks can record the orientation of the magnetic field at the time of
511 magnetization (e.g. Tauxe, 2010). The magnetic vector can be geometrically defined by two
512 components: inclination, which is a function of the paleolatitude (being 90° at the poles and 0° at
513 the equator) at the time of magnetization acquisition; and declination, which is a measure of the
514 horizontal angular difference between the recorded magnetic direction and true north, thereby
515 allowing for the quantification of any vertical-axis rotations if a reference paleomagnetic pole is
516 known for the region of interest at the time of magnetization acquisition. Paleomagnetism is the
517 best tool to quantify vertical-axis rotations in orogens due to the independence of the magnetic
518 field from an orogen's deformation and evolution (e.g. Butler, 1998).

519 Despite its uniqueness to study paleolatitudes and vertical-axis rotations,
520 paleomagnetism is not flawless. Paleomagnetic data can yield spurious rotations when the local
521 and regional structures are not properly defined and their geometries and kinematic histories not
522 adequately corrected for (e.g. Pueyo et al., 2016). In addition, the age of magnetization
523 acquisition is not necessarily equivalent to the age of the sampled rock. Remagnetizations are
524 ubiquitous, especially in orogens (Weil and van der Voo, 2002; Pueyo et al., 2007; Huang et al.,
525 2017). In remagnetized rocks, the primary magnetization is replaced or overprinted due to a set
526 of geologic processes acting alone or in concert - usually represented by a combination of
527 thermal or chemical reactions (e.g., Jackson, 1990). Nevertheless, remagnetizations can be
528 useful for interpreting deformation history if the relative timing of the overprint can be
529 established and a well-constrained reference direction for that age is known (e.g. Weil et al.,
530 2001; Izquierdo-Llavall et al. 2015; Calvin et al., 2017).

531 In addition to knowing the structural geology and the timing of magnetization of the
532 studied rocks, understanding and quantifying local and regional vertical-axis rotations requires a
533 paleomagnetic reference pole for comparison. Permian and Mesozoic paleomagnetic studies in
534 Iberia indicate that Iberia was a relatively stable plate from at least Guadalupian times (ca. 270
535 Ma) to the opening of the Bay of Biscay in the Cretaceous (e.g. Gong et al., 2008; Vissers et al.,
536 2016). Weil et al. (2010) calculated the an Early Permian pole for stable Iberia, which will be
537 used herein as a reference for any vertical-axis rotation analysis (hereafter, eP pole or eP
538 component). Weil et al.'s Virtual Geomagnetic Pole (VGP) values are $Plat = 43.9$; $Plong = 203.3$
539 and $\alpha_{95} = 5.4$ and when transform into paleomagnetic components has a $\sim 0^\circ$ inclination

540 (equatorial) and declinations that range from 150° to 160° (from NW to SW respectively)
541 depending on where in Iberia you are referencing. In Fig. 6 (red arrows), a compilation of
542 declinations that form part of this composite pole and other eP components found in recent
543 studies are presented.

544 For the Central Iberian curve, the voluminous paleomagnetic database from the
545 Cantabrian Orocline can be used to partially constrain its kinematics (e.g. Weil et al., 2013). The
546 orocline test for the Cantabrian Orocline (Fig. 4) quantifies the degree of differential vertical-axis
547 rotation of variously striking Variscan tectonic belts in northern Iberia. If the Central Iberian
548 curve is a product of vertical-axis rotation, paleomagnetic declinations would bend around the
549 Central Iberian curve opposite to that of the Cantabrian Orocline. With a well constrained
550 orocline test, as in the Cantabrian Orocline (Fig. 4), one can use the paleomagnetic strike-test
551 correlation slope to establish expected declinations for any along-strike portion of the orogen
552 (Pastor-Galán et al., 2017b).

553 Before the resurgence of the Central Iberian curve, the only available pre-Permian
554 paleomagnetic studies to the south and west of the Cantabrian Zone in the Iberian Massif were
555 from the Beja Gabbroic Massif, Portugal (Perroud et al., 1985) and the Almadén syncline
556 volcanics (Perroud et al., 1991; Pares & Van der Voo, 1992). The Beja area study presented
557 varied inclinations and declinations in the gabbros, and complex overprints elsewhere. Perroud
558 et al. (1985) did not consider any structural correction for the results, as they assumed the
559 gabbro was undeformed. Recently, Dias da Silva et al. (2018) showed that the area underwent
560 intense deformation during the Carboniferous. Therefore, interpretation of this dataset is
561 complicated without knowing the proper structural correction needed to restore the
562 magnetization to its palinspastic orientation.

563 Several articles with new paleomagnetic studies around the Central Iberian curve have
564 been published since 2015 (Fig. 6). In general, these studies have reported a pervasive late
565 Carboniferous (320 to 300 Ma) (re-)magnetization in sedimentary and igneous rocks (e.g.
566 Pastor-Galán et al., 2015a; 2017b; Fernández-Lozano et al. 2016), which is largely
567 penecontemporaneous to the intrusion of E1 extensional granites (López-Moro et al., 2018) and
568 C3 syn-orocline mantle derived granitoids (Fig. 2C; e.g. Gutiérrez-Alonso et al., 2011a). The
569 following section describes the reported magnetizations from oldest to youngest.

570 Pastor-Galán et al. (2016) sampled for paleomagnetic analyses both E1 extensional
571 granites (Fig. 2C; ~320 Ma; e.g. López-Moro et al., 2018) from the Tormes and Martinamor
572 domes, and C3 mantle derived granitoids from the Central System (Fig. 2C; 305-295 Ma; e.g.
573 Gutiérrez-Alonso et al., 2011a). Both sets of plutons are located around the Galicia Tras-os-

574 Montes hinge of the Central Iberian curve (Fig. 6-5). The authors found an original component in
575 E1 granites supported by a positive reversal test in both domes (Fig. 7). The magnetization has
576 an inclination (Inc.) = 15° (paleolatitude (λ) = -7.6°) and declination (Dec.) = 81° (Fig. 7), which
577 imply a northward movement of 700 km and a ~70° CCW rotation with respect to the C3
578 granites that showed an eP component (Dec. ~ 150, Inc. ~ 0). Considering the positive reversal
579 test in E1 granites and the significant difference in inclinations with respect to C3 granitoids (eP
580 component), a magnetization age of older than 318 Ma was proposed (pre-Kiaman superchron,
581 317 Ma - 267 Ma, e.g. Langereis et al., 2010), which was interpreted as a primary
582 magnetization. The 70° CCW Pennsylvanian rotation recorded in rocks from the Central Iberian
583 curve hinge zone is in agreement with the expected rotation of the southern limb of the
584 Cantabrian Orocline (Fig. 4; Weil et al., 2013).

585 At the putative outer arc of the Central Iberian curve in the Iberian Ranges (Fig. 2),
586 paleomagnetic and structural studies of Devonian and Permian rocks (Pastor-Galán et al.,
587 2018) revealed that the eP component from Permian rocks had rotated ~22° CW during the
588 Cenozoic (Fig. 8; cf. Pastor-Galán et al., 2018). The Permian and Mesozoic rocks from the
589 Iberian Ranges show a consistent ~22° CW rotation with respect to the Apparent Polar Wander
590 Path for Iberia (e.g. Pastor-Galán et al. 2018). This rotation likely happened during the Alpine
591 orogeny, in which the northern area of the Iberian Range underwent more shortening than the
592 southern part, resulting in a regional CW vertical-axis rotation (Izquierdo-Llavall et al., 2019).
593 After restoring the Cenozoic rotation, the Devonian rocks show a positive reversal and fold-test
594 with inclinations that are steeper than expected from the eP component (Dec. = 85.3°, Inc. =
595 12.7°, λ = -6.4). This component is statistically indistinguishable from that of the E1 granites and
596 the southern branch of the Cantabrian Zone, showing the same 70° CCW rotation from the time
597 they were remagnetized (estimated ~318 Ma) to the timing of the eP component (Fig. 8; Pastor-
598 Galán et al., 2018). Once Cenozoic rotation is corrected for, the structural and paleomagnetic
599 trends of the Iberian ranges become parallel to those in the southern limb of the Cantabrian
600 Orocline, ruling out a Variscan or older origin for the outer Central Iberian curve (Fig. 8).

601 The remaining paleomagnetic works published on Central and SW Iberia rocks all reveal
602 a ubiquitous late Carboniferous to Early Permian remagnetization during the Kiaman
603 superchron (Fernández-Lozano et al., 2016; Pastor-Galán et al., 2015a; 2016; 2017b; Leite
604 Mendes, in press). The authors of these papers calculated the expected declination for each
605 site as if they were part of the Cantabrian Orocline (Fig. 9A). All localities where magnetizations
606 pre-date the formation of the Cantabrian Orocline show the same expected rotations as the
607 southern limb of the Cantabrian Orocline, regardless of their position within the Central Iberian

608 curve (to the hinge: Tormes and Martinamor domes, Iberian ranges; to the southern limb:
609 Almadén syncline and South Portuguese Zone). Other locations, especially limestones from the
610 Central Iberian Zone, have declinations and inclinations in between the primary 318 Ma
611 component of the E1 granites and the post-orocline eP component (Fig. 9B). Pastor-Galán et al.
612 (2015a; 2016) interpreted these results as being caused by a remagnetization that was acquired
613 during formation of the Cantabrian Orocline and therefore record intermediate steps between
614 the component of the E1 granites and eP. Those authors suggest that the large amount of syn-
615 orocline mantle derived granitoids that intruded the Central Iberian Zone (C3 granitoids)
616 triggered the hinterland remagnetization.

617 Finally, two previous studies identified an earlier magnetization in the Almadén syncline
618 region of the SE Central Iberian Zone (Perroud et al., 1991; Pares & Van der Voo, 1992).
619 However, Leite Mendes et al. (in press) argue that these studies are likely misinterpreted.
620 Perroud et al. (1991), applied a complicated structural correction restoring a putative plunge of
621 the regional structural axis to all sites, including those where the syncline axis does not plunge.
622 Leite Mendes et al. (in press) re-sampled the syncline where its axis is sub-horizontal and
623 obtained a negative fold test, implying that the magnetization is not primary as previously
624 interpreted. Their results, however, are similar in orientation to those components published
625 from previous studies prior to any structural correction (Perroud et al., 1991 and Parés and van
626 der Voo, 1992).

627 Two additional studies sampled Laurussian margin sequences that are today adjacent to
628 the Cantabrian Orocline region (Fig. 10). To the north, the SW part of Ireland preserves a Late
629 Paleozoic basin filled with Devonian red sandstone and Carboniferous limestone and siltstone,
630 which was sampled by Pastor-Galán et al. (2015a). To the south are the aforementioned results
631 from the South Portuguese Zone (Leite Mendes et al., in press). Both areas are interpreted to
632 have previously been part of the Laurussian continent, and therefore on the opposite side of the
633 Rhenish Ocean suture at the time of Variscan collision (Fig. 10; e.g. Pastor-Galán et al., 2015b). In
634 contrast, the rest of Iberia was part of, or proximal to, Gondwana (e.g. Franke et al., 2017).
635 These Paleomagnetic results from the Laurussian margin suggest that the rotations involved in
636 the formation of the Cantabrian Orocline occurred along both sides of the Rhenish suture along its
637 northern and southern limbs (Fig. 10A and B). Pastor-Galán et al. (2015b) hypothesized a so-
638 called Greater Cantabrian Orocline that would have bent the entire Appalachian/Variscan
639 orogen around a vertical-axis, affecting at least the continental margins of both Gondwana and
640 Laurussia.

641 5.3 The implications of not being a secondary orocline

642 The most relevant new data regarding the kinematics of the Central Iberian curve is the
643 paleomagnetic study from the Iberian Ranges (Calvín et al., 2014; Pastor-Galán et al., 2018).
644 These results confirm that the present-day variation in trend of the tectonostratigraphic units,
645 generally attributed to Variscan tectonics (e.g. Weil et al., 2013; Shaw et al., 2012; 2014), is
646 likely a product of Cenozoic Alpine orogeny. Izquierdo-Llavall et al. (2019) confirmed that the
647 interpreted Alpine rotations correspond well with the amount of shortening reconstructed in
648 Meso-Cenozoic basins. The best preserved and most continuous outcrop in the Central
649 Iberian's outer arc is not a Variscan structure, casting doubt that the Central Iberian curve is
650 related to Variscan kinematics. These results are also a reminder that the regional effects of
651 Alpine deformation are often underestimated, especially close to the major Iberian Alpine fronts:
652 the Pyrenees, Iberian Ranges, and the Betics.

653 Overall, new paleomagnetic data from the Central Iberian curve and nearby areas reveal
654 pervasive late Carboniferous remagnetizations and regional vertical-axis rotations of the same
655 sense and magnitude to those expected for the southern arm of the Cantabrian Orocline. The
656 new paleomagnetic data indicate that a post ~320 Ma formation for the Central Iberia curve due
657 to vertical-axis rotations is not supported (Pastor-Galán et al., 2016). The distribution in space
658 and time of paleomagnetic results makes it unlikely that the formation of the Central Iberian
659 curve is a product of Variscan gravitational collapse (E1, ~330-317 Ma) or concomitant to the
660 Cantabrian Orocline (C3). So far, no pre-E2 paleomagnetic component has been found, and
661 consequently, paleomagnetic data cannot reject an early orogenic origin for the inner arc of the
662 Central Iberian curve (C1-C2, older than 330 Ma).

663 From a structural geology point of view, the Central Iberian curve does not display the
664 classic geometries and structural interference patterns found in other established oroclines (i.e.,
665 those systems that involve differential vertical-axis rotations, e.g. Li et al., 2012; van der Boon et
666 al., 2018; Meijers et al., 2017; Rezaeian et al., 2020). The geometry and structural behavior of
667 oroclines should resemble, at the crustal-scale, a regional vertical-axis fold preserved in plan-
668 view, either formed by buckling (e.g. Johnston et al., 2001) or bending (e.g. Cifelli et al., 2008)
669 mechanisms. In oroclines, pre-existing structures tend to follow fold trends around the curvature
670 (e.g. Rosenbaum, 2014; Li et al., 2018). In addition, orocline cores tend to preserve radial
671 structures and shortening patterns in the inner arc and orocline parallel shear zones and
672 extensional structures in their outer arc (e.g. Ries and Shackleton, 1976; Eichelberger and
673 McQuarrie, 2015), similar to what is observed in multilayer folds (e.g. Fossen, 2016).

674 The structural geometry of the Central Iberian curve lacks such patterns.

675 Paleomagnetism from the Iberian Ranges indicate that the Cantabrian and West Asturian
676 Leonese zones do not follow the Central Iberian curve, instead they continue their WNW-ESE
677 trend into the Mediterranean in what it is now the Betic chain (Rodríguez-Cañero et al., 2018;
678 Jabaloy-Sánchez et al., 2018; van Hinsbergen et al., 2020). Structural trends in the Ossa
679 Morena and the South Portuguese Zone do not show any change in along-strike structural trend
680 that supports large-scale CW rotations (e.g. Pérez-Cáceres et al., 2015; Quesada et al., 2019),
681 whereas existing paleomagnetic data from those zones (Leite Mendes et al., in press) support a
682 model of CCW rotation associated with the broader southern arm of the Cantabrian Orocline. In
683 the Central Iberian and Galicia Tras-os-Montes zones, the trend of curvature is irregular (see C1
684 fold patterns in Fig. 2A) and nowhere are the expected inner and outer arc-related structures
685 preserved (e.g. Dias da Silva et al., 2020).

686 The curved shape of C1 fold axes in the Central Iberian Zone is better explained by fold
687 interference patterns than vertical-axis rotations (e.g. Pastor-Galán et al., 2019b). Moreover, the
688 curved shape of the Galicia Tras-os-Montes allochthonous nappe, which was emplaced orogen-
689 parallel, shows no evidence of vertical-axis rotation related structures (Fig. 2A; Dias da Silva et
690 al., 2020). Other authors describe the changes in trend around the Central Iberian curve
691 expressed by C1 folds (Fig. 2A) as the product of fold interference patterns (e.g. Gutiérrez-
692 Alonso, 2009; Palero-Fernández et al., 2015; Jacques et al., 2018b; Dias da Silva et al., 2020).
693 Pastor-Galán et al. (2019b) showed that curved C1 folds in the Central Iberian Zone around the
694 Galicia Tras-os-Montes boundary (Fig. 2A) are coaxial with C3 folds after restoring the effects of
695 C2 and E1 deformation phases. Both C1 and C3 structures formed under similar shortening
696 directions. In the same area, Jacques et al. (2018b) found similar fold interference patterns, in
697 addition they described kinematic incompatibility with the expected CW rotations that would
698 have occurred if the Central Iberian curve were an orocline. In other areas of the Central Iberian
699 Zone, the curved shape of C1 folds has been described as an interference between C1
700 structures and their reorientation caused by C3 shear zones (Fig. 2A; e.g. Palero-Fernández et
701 al., 2015; Dias et al., 2016), or alternatively the interference between C1, C3 and the E2
702 structures (Fig. 2A; Gutiérrez-Alonso, 2009; Arango et al., 2013; Rubio Pascual et al. 2013).

703 Overall, new geometric and kinematic data favor the interpretation that the Central
704 Iberian curve is not a structure formed by differential vertical-axis rotation as was the Cantabrian
705 Orocline, but one formed as a consequence of several competing processes. It is clear from the
706 current data that a combination of several deformation events caused the orientation of
707 structures that today delineate the shape of the Central Iberia curve. These include: (1) the
708 northern part of the outer-arc as the product of an Alpine rigid block rotation instead of Variscan

709 differential vertical-axis rotation (Pastor-Galán et al., 2018); (2) the curvature of the Galicia Tras-
710 os-Montes allochthonous nappe reflects its original shape and could be defined as a primary
711 curve (see Weil and Sussman, 2004), since it was emplaced orogen parallel and preserves no
712 evidence of vertical-axis rotations (fig. 2A; Dias da Silva et al., 2020); (3) Structural analysis
713 shows that fold interference patterns explain the geometry of the curved trends of Central
714 Iberian Zone's C1 folds (Pastor-Galán et al., 2019b), whose kinematics are incompatible with
715 the required CW rotations expected if the curve is an orocline (Jacques et al, 2018b).

716 6 Get Back: Ideas flowing out and endless questions

717 The pioneering works in the last decade that resurrected the idea of a Central Iberian
718 curve, speculated that both the Cantabrian and Central Iberian zones buckled together as
719 secondary oroclines (Fig. 11; Martínez-Catalán 2011; Shaw et al., 2012, 2014; Shaw and
720 Johnston, 2016; Carreras and Druguet, 2014). Later, Martínez Catalan et al. (2014) and Díez
721 Fernández and Pereira (2017) reformulated Martínez-Catalán's 2011 hypothesis and proposed
722 that the Central Iberian curve formed as an orocline between 315 and 305 Ma, and assigning
723 the Cantabrian Orocline a time frame between 305 and 295 Ma (Fig. 11). The proposed tectonic
724 mechanisms to support these early kinematic models are varied: (1) buckling of a ribbon
725 'Armorican' continent (Fig. 11A; Shaw et al., 2014; 2016); (2) buckling of a completely formed
726 Variscan orogen during a putative 'Pangea B' to 'Pangea A' transition in the late Carboniferous
727 (Fig. 11B; Carreras and Druguet, 2014; Martínez-Catalán et al., 2011); (3) indentation of
728 Laurussia into Gondwana during the early stages of collision (at present day SW Iberia, South
729 Portuguese Zone), producing first the Central Iberian curve as a mega drag-fold during
730 Carboniferous times and then slightly later the Cantabrian Orocline as a consequence of an
731 indentation process (Fig. 11C; Simancas et al., 2013).

732 The reviewed data in sections 4 and 5 contradict the aforementioned hypotheses.
733 Paleomagnetism and structural patterns (section 5; Fig. 6-11) disagree with the necessary CW
734 rotations required to support a late Carboniferous orocline origin for the Central Iberian curve
735 (Models in Fig. 11A and B). In addition, the sense and magnitude of the vertical-axis rotations
736 observed in SW Iberia (Fig. 10) imply that the South Portuguese (Avalonian segment) and Ossa
737 Morena zones moved together with the southern limb of the Cantabrian Orocline during the
738 Pennsylvanian and Early Permian. This means that the South Portuguese Zone was already
739 parallel to the general trend of the Variscan orogen prior to Cantabrian Orocline formation,
740 implying the lack of a Laurussian rigid indenter into Gondwana (e.g. Simancas et al., 2013). This
741 discrepancy leaves orogen-parallel terrane transport as a possible explanation to the kinematics

742 observed in the Ossa Morena and South-Portuguese zones (e.g. Pérez-Cáceres et al., 2016).
743 At the same time, paleomagnetism from SW Iberia supports the hypothesis of a Greater
744 Cantabrian Orocline that extended into both Gondwana and Laurussia in its northern and
745 southern limbs (Fig. 10; Pastor-Galán et al., 2015b).

746 In spite of the kinematic constraints and structural patterns that do not support a vertical-
747 axis origin for the Central Iberian curve in Late Carboniferous time, there are geometric
748 constraints that remain challenging to account for. For example, the curved shape of the
749 aeromagnetic and gravity anomalies of Iberia are real (Fig. 5). These striking patterns could be
750 due to Variscan-Alpine structural interference, as suggested for the Iberian Ranges, but
751 currently there is not enough data to rigorously test this hypothesis. In addition are the curved
752 traces of C1 fold-axes, whose geometry and kinematics are reasonably well constrained around
753 Galicia Tras-os-Montes (e.g. Dias da Silva et al., 2020), but in many other areas their strong
754 curvature remain largely unstudied (Fig. 2) and therefore, to date we can only speculate on their
755 origin.

756 Shaw et al. (2012) supported their hypothesis of a secondary orocline by assuming that
757 paleocurrents were parallel through Iberia during Ordovician times. However, some of the
758 observed deflections in the paleocurrents studied by Shaw et al. (2012; see Fig. 3) are also
759 explained by Alpine vertical-axis rotations (the case of the Iberian ranges) and fold interference
760 patterns (SE of the Central Iberian Zone). Others (Central and SW of the Central Iberian Zone)
761 may be explained by a local response to basin architecture (Fig. 3), where paleo-flow directions
762 would trend toward the deepest basin troughs. The Ordovician basin architecture of Iberia
763 allows for opposite directed paleocurrents from both sides of such troughs (Fig. 3). However,
764 the Early Paleozoic basin architecture in Iberia and their local deformation events require further
765 research (Sánchez-García et al., 2019).

766 Finally, although kinematic evidence is still scarce for the earliest pre-Variscan and early
767 Variscan events, we argue that pre-orogenic physiographic features, such as the opening of a
768 marginal restricted ocean between Gondwana and its distal platform at 395 Ma (Fig. 12A; Pin et
769 al., 2002; Gutiérrez-Alonso et al., 2008b; Arenas et al., 2016) explains the rounded shape of the
770 Galicia Tras-os-Montes curve as a primary curve. During collision, the latter irregularity would
771 cause the orogen-parallel emplacement of allochthonous nappes (Fig. 12B; Dias da Silva et al.,
772 2020) and the sinistral movements of the Ossa Morena and South Portuguese zones in SW
773 Iberia (Fig 13A, B, C; Quesada, 2019). During the late Carboniferous, possibly due to a plate
774 reorganization during the final amalgamation of Pangea (Fig. 12D; e.g. Gutiérrez-Alonso et al.,
775 2008a; Pastor-Galán et al., 2015a), the far-field stress-field likely changed, which caused the

776 entire orogen to buckle around a vertical axis (Gutiérrez-Alonso et al., 2004), including both the
777 Gondwana and Laurussia margins (Fig. 12E; Pastor-Galán et al., 2015b).

778 Author contribution

779 DPG is responsible for Data curation and Visualization in the paper. All authors contributed
780 equally to discussion of ideas and manuscript writing at all stages.

781 Acknowledgements

782 DPG thanks the extraordinary hard work, patience and endurance of the Utrecht
783 University students that embraced and enjoyed studying the kinematics of the Central Iberian
784 curve: Thomas Groenewegen, Bart Ursem, Daniel Brower, Mark Diederer and Bruno Leite-
785 Mendes. DPG acknowledges FRIS and CNEAS for the continuous financial support. GGA is
786 supported by Spanish Ministry of Science, innovation and universities under the project
787 IBERCRUST (PGC2018-096534-B-I00) and Russian Federation Government grant no.
788 14.Y26.31.0012. This paper is a contribution to the IGCP no. 648 “Supercontinent Cycles and
789 Global Geodynamics”. 50 years ago four fabulous guys let it be and never got back.

790 Competing interests

791 The authors declare that they have no conflict of interest.

792 References

- 793 Ábalos, B., Carreras, J., Druguet, E., Escuder Viruete, J., Gómez Pugnairé, M. T., Lorenzo
794 Álvarez, S., Quesada, C., Rodríguez Fernández, L. R. and Gil-Ibarguchi, J. I.: Variscan and pre-
795 Variscan tectonics, *Geol. Spain*, 155–183, 2002.
- 796 Aerden, D.: Correlating deformation in Variscan NW-Iberia using porphyroblasts; implications for
797 the Ibero-Armorican Arc, *J. Struct. Geol.*, 26(1), 177–196, 2004.
- 798 Alcock, J. E., Catalán, J. R. M., Arenas, R. and Montes, A. D.: Use of thermal modeling to
799 assess the tectono-metamorphic history of the Lugo and Sanabria gneiss domes, Northwest
800 Iberia, *Bull. Société Géologique Fr.*, 180(3), 179–197, doi:10.2113/gssgfbull.180.3.179, 2009.
- 801 Aller, J., Bastida, F. and Bobillo-Ares, N. C.: On the development of kink-bands: A case study in
802 the West Asturian-Leonese Zone (Variscan belt, NW Spain) / Sur le développement des kink-
803 bands : un exemple dans le Zone Astur Occidentale-léonaise (chaîne varisque ibérique, nord-
804 ouest de l'Espagne), *Bull. Société Géologique Fr.*, 191(1), doi:10.1051/bsgf/2020003, 2020.
- 805 Aller, J. J. J. and Gallastegui, J. J.: Analysis of kilometric-scale superposed folding in the
806 Central Coal Basin (Cantabrian zone, NW Spain), *J. Struct. Geol.*, 17(7), 961–969,

- 807 doi:10.1016/0191-8141(94)00115-G, 1995.
- 808 Alonso, J. L., Marcos, A. and Suárez, A.: Paleogeographic inversion resulting from large out of
809 sequence breaching thrusts: The León Fault (Cantabrian zone, NW Iberia). A new picture of the
810 external Variscan thrust belt in the Ibero-Armorican arc, *Geol. Acta*, 7(4), 451–473,
811 doi:10.1344/105.000001449, 2009.
- 812 Álvaro, J. J., Casas, J. M., Clausen, S. and Quesada, C.: Early Palaeozoic geodynamics in NW
813 Gondwana, *J. Iber. Geol.*, 44(4), 551–565, doi:10.1007/s41513-018-0079-x, 2018.
- 814 Ardizzone, Juan, Julio Mezcua, and Isabel Socías. Mapa aeromagnético de España peninsular.
815 Instituto Geográfico Nacional, 1989.
- 816 Mergl, M. & Zamora, S. 2012, New and revised occurrences of... *Bulletin of Geosciences*, 87,
817 571-586., [online] Available from: <http://www.geology.cz/bulletin/contents/art1327> (Accessed 6
818 April 2020b), n.d.
- 819 Aramburu, C., Méndez-Bedia, I. and Arbizu, M.: The Lower Palaeozoic in the Cantabrian Zone
820 (Cantabrian Mountains, NW Spain)., edited by S. García-López and F. Bastida, pp. 35–49.,
821 2002.
- 822 Arango, C., Díez Fernández, R. and Arenas, R.: Large-scale flat-lying isoclinal folding in
823 extending lithosphere: Santa María de la Alameda dome (Central Iberian Massif, Spain),
824 *Lithosphere*, 5(5), 483–500, doi:10.1130/L270.1, 2013.
- 825 Arenas, R., Sánchez Martínez, S., Díez Fernández, R., Gerdes, A., Abati, J., Fernández-
826 Suárez, J., Andonaegui, P., González Cuadra, P., López Carmona, A., Albert, R., Fuenlabrada,
827 J. M. and Rubio Pascual, F. J.: Allochthonous terranes involved in the Variscan suture of NW
828 Iberia: A review of their origin and tectonothermal evolution, *Earth-Sci. Rev.*, 161, 140–178,
829 doi:10.1016/j.earscirev.2016.08.010, 2016.
- 830 Ayala, C., Bohoyo, F., Maestro, A., Reguera, M. I., Torne, M., Rubio, F., Fernández, M. and
831 García-Lobón, J. L.: Updated Bouguer anomalies of the Iberian Peninsula: a new perspective to
832 interpret the regional geology, *J. Maps*, 12(5), 1089–1092,
833 doi:10.1080/17445647.2015.1126538, 2016.
- 834 Ayarza, P., Catalan, J. R. M., Gallart, J., Pulgar, J. A. and Danobeitia, J. J.: Estudio Sísmico de
835 la Corteza Iberica Norte 3.3: A seismic image of the Variscan crust in the hinterland of the NW
836 Iberian Massif, *Tectonics*, 17(2), 171–+, 1998.
- 837 Azor, A., Rubatto, D., Simancas, J. F., Lodeiro, F. G., Poyatos, D. M., Parra, L. M. M. and
838 Matas, J.: Rheic Ocean ophiolitic remnants in Southern Iberia questioned by SHRIMP U-Pb
839 zircon ages on the Beja-Acebuches amphibolites - art. no. TC5006, *Tectonics*, 27(5), C5006–
840 C5006, 2008.
- 841 Azor, A., Dias da Silva, Í., Gómez Barreiro, J., González-Clavijo, E., Martínez Catalán, J. R.,
842 Simancas, J. F., Martínez Poyatos, D., Pérez-Cáceres, I., González Lodeiro, F., Expósito, I.,
843 Casas, J. M., Clariana, P., García-Sansegundo, J. and Margalef, A.: Deformation and Structure,
844 in *The Geology of Iberia: A Geodynamic Approach*, edited by C. Quesada and J. T. Oliveira, pp.
845 307–348, Springer International Publishing, Cham., 2019.

- 846 Barrois, C. E.: Recherches sur le terrains anciens des Asturies et de la Galice, Six-Horemans.,
847 1882.
- 848 Bastida, F.: Zona Cantábrica, in *Geología de España*, edited by J. A. Vera, pp. 25–49, SGE-
849 IGME, Madrid., 2004.
- 850 Bayona, G., Thomas, W. A. and Van der Voo, R.: Kinematics of thrust sheets within transverse
851 zones: A structural and paleomagnetic investigation in the Appalachian thrust belt of Georgia
852 and Alabama, *J. Struct. Geol.*, 25(8), 1193–1212, doi:10.1016/S0191-8141(02)00162-1, 2003.
- 853 van der Boon, A., van Hinsbergen, D. J. J. J., Rezaeian, M., Gürer, D., Honarmand, M.,
854 Pastor-Galán, D., Krijgsman, W. and Langereis, C. G. G.: Quantifying Arabia–Eurasia
855 convergence accommodated in the Greater Caucasus by paleomagnetic reconstruction, *Earth
856 Planet. Sci. Lett.*, 482, doi:10.1016/j.epsl.2017.11.025, 2018.
- 857 Buitter, S. J. H. and Torsvik, T. H.: A review of Wilson Cycle plate margins: A role for mantle
858 plumes in continental break-up along sutures?, *Gondwana Res.*, 26(2), 627–653,
859 doi:10.1016/j.gr.2014.02.007, 2014.
- 860 Butler, R.: Paleomagnetism: Magnetic domains to geologic terranes, *Electron. Ed.*,
861 (September), 319–319, doi:10.1006/icar.2001.6754, 1998.
- 862 Calvin, P., Casas, A. M., Villalaín, J. J., Tierz, P., Calvin, P., Casas, A. M., Villalaín, J. J., Tierz,
863 P., Calvin, P., Casas, A. M., Villalaín, J. J. and Tierz, P.: Reverse magnetic anomaly controlled
864 by Permian Igneous rocks in the Iberian Chain (N Spain), *Geol. Acta*, 12(3), 193–207,
865 doi:10.1344/GeologicaActa2014.12.3.2, 2014.
- 866 Calvin, P., Casas-Sainz, A. M. M., Villalaín, J. J. J. and Moussaid, B.: Diachronous folding and
867 cleavage in an intraplate setting (Central High Atlas, Morocco) determined through the study of
868 remagnetizations, *J. Struct. Geol.*, 97, 144–160, doi:10.1016/j.jsg.2017.02.009, 2017.
- 869 Calvin-Ballester, P. and Casas, A.: Folded Variscan thrusts in the Herrera Unit of the Iberian
870 Range (NE Spain), *Geol. Soc. Lond. Spec. Publ.*, 394(1), 39–52, doi:10.1144/SP394.3, 2014.
- 871 Carey, S. W.: The orocline concept in geotectonics-Part I, *Pap. Proc. R. Soc. Tasman.*, 89,
872 255–288, 1955.
- 873 Carreras, J. and Druguet, E.: Framing the tectonic regime of the NE Iberian Variscan segment,
874 *Geol. Soc. Lond. Spec. Publ.*, 405(1), 249–264, doi:10.1144/SP405.7, 2014.
- 875 Chopin, F., Schulmann, K., Skrzypek, E., Lehmann, J., Dujardin, J. R., Martelat, J. E., Lexa, O.,
876 Corsini, M., Edel, J. B., Štípská, P. and Pitra, P.: Crustal influx, indentation, ductile thinning and
877 gravity redistribution in a continental wedge: Building a Moldanubian mantled gneiss dome with
878 underthrust Saxothuringian material (European Variscan belt), *Tectonics*, 31(1), n/a-n/a,
879 doi:10.1029/2011TC002951, 2012.
- 880 Chopin, F., Corsini, M., Schulmann, K., El Houicha, M., Ghienne, J.-F. and Edel, J.-B.: Tectonic
881 evolution of the Rehamna metamorphic dome (Morocco) in the context of the Alleghanian-
882 Variscan orogeny, *Tectonics*, 33(6), 1154–1177, doi:10.1002/2014TC003539, 2014.
- 883 Cifelli, F., Mattei, M. and Della Seta, M.: Calabrian Arc oroclinal bending: The role of subduction,

- 884 Tectonics, 27(5), doi:10.1029/2008TC002272, 2008.
- 885 Dallmeyer, R. D., Fonseca, P. E., Quesada, C. and Ribeiro, A.: 40Ar/39Ar mineral age
886 constraints for the tectonothermal evolution of a Variscan suture in southwest Iberia,
887 Tectonophysics, 222(2), 177–194, doi:10.1016/0040-1951(93)90048-O, 1993.
- 888 Dallmeyer, R. D. D., Catalán, J. R. M., Arenas, R., Gil Ibarra, J. I. I., Gutiérrez-Alonso, G.,
889 Farias, P., Bastida, F. and Aller, J.: Diachronous Variscan tectonothermal activity in the NW
890 Iberian Massif: Evidence from 40Ar/39Ar dating of regional fabrics, Tectonophysics, 277(4),
891 307–337, doi:10.1016/S0040-1951(97)00035-8, 1997.
- 892 Dias da Silva, Í., Gómez-Barreiro, J., Martínez Catalán, J. R., Ayarza, P., Pohl, J. and Martínez,
893 E.: Structural and microstructural analysis of the Retortillo Syncline (Variscan belt, Central
894 Iberia). Implications for the Central Iberian Orocline, Tectonophysics, 717, 99–115,
895 doi:10.1016/j.tecto.2017.07.015, 2017.
- 896 Dias da Silva, Í., Pereira, M. F., Silva, J. B. and Gama, C.: Time-space distribution of silicic
897 plutonism in a gneiss dome of the Iberian Variscan Belt: The Évora Massif (Ossa-Morena Zone,
898 Portugal), Tectonophysics, 747–748, 298–317, doi:10.1016/j.tecto.2018.10.015, 2018.
- 899 Dias da Silva, Í., González Clavijo, E. and Díez-Montes, A.: The collapse of the Variscan belt: a
900 Variscan lateral extrusion thin-skinned structure in NW Iberia, Int. Geol. Rev., 00(00), 1–37,
901 doi:10.1080/00206814.2020.1719544, 2020.
- 902 Dias da Silva, Í. F., Linnemann, U., Hofmann, M., González-Clavijo, E., Díez-Montes, A. and
903 Catalán, J. R. M.: Detrital zircon and tectonostratigraphy of the Parautochthon under the Morais
904 Complex (NE Portugal): implications for the Variscan accretionary history of the Iberian Massif,
905 J. Geol. Soc., 172(1), 45–61, doi:10.1144/jgs2014-005, 2015.
- 906 Dias, R. and Ribeiro, A.: Finite strain analysis in a transpressive regime (Variscan autochthon,
907 northeast Portugal), Tectonophysics, 191(3), 389–397, doi:10.1016/0040-1951(91)90069-5,
908 1991.
- 909 Dias, R. and Ribeiro, A.: CONSTRICTION IN A TRANSPRESSIVE REGIME - AN EXAMPLE IN
910 THE IBERIAN BRANCH OF THE IBERO-ARMORICAN ARC, J. Struct. Geol., 16(11), 1543–
911 1554, 1994.
- 912 Dias, R., Mateus, A., and Ribeiro, A., Strain partitioning in transpressive shears zones in the
913 southern branch of the Variscan Ibero-Armorican arc: Geodinamica Acta, v. 16, no. 2–6, p. 119–
914 129. doi:10.1016/j.geoact.2003.04.001, 2003.
- 915 Dias, R., Ribeiro, A., Romão, J., Coke, C. and Moreira, N.: A review of the arcuate structures in
916 the Iberian Variscides; constraints and genetic models, Tectonophysics, 681, 170–194,
917 doi:10.1016/j.tecto.2016.04.011, 2016.
- 918 Díez Balda, M. A., Vegas, R. and González Lodeiro, F.: Central-Iberian zone structure, Pre-
919 Mesoz. Geol. Iber., 172–188, 1990.
- 920 Díez Balda, M. A., Martínez Catalán, J. R. and Ayarza Arribas, P.: Syn-collisional extensional
921 collapse parallel to the orogenic trend in a domain of steep tectonics: the Salamanca
922 Detachment Zone (Central Iberian Zone, Spain), J. Struct. Geol., 17(2), 163–182,

- 923 doi:10.1016/0191-8141(94)E0042-W, 1995.
- 924 Díez Fernández, R. and Arenas, R.: The Late Devonian Variscan suture of the Iberian Massif: A
925 correlation of high-pressure belts in NW and SW Iberia, *Tectonophysics*, 654, 96–100,
926 doi:10.1016/j.tecto.2015.05.001, 2015.
- 927 Díez Fernández, R. and Pereira, M. F.: Extensional orogenic collapse captured by strike-slip
928 tectonics: Constraints from structural geology and UPb geochronology of the Pinhel shear zone
929 (Variscan orogen, Iberian Massif), *Tectonophysics*, 691, 290–310,
930 doi:10.1016/j.tecto.2016.10.023, 2016.
- 931 Díez Fernández, R. and Pereira, M. F.: Strike-slip shear zones of the Iberian Massif: Are they
932 coeval?, *Lithosphere*, 9(5), 726–744, doi:10.1130/L648.1, 2017.
- 933 Díez Fernández, R., Gómez Barreiro, J., Martínez Catalán, J. R. and Ayarza, P.: Crustal
934 thickening and attenuation as revealed by regional fold interference patterns: Ciudad Rodrigo
935 basement area (Salamanca, Spain), *J. Struct. Geol.*, 46, 115–128,
936 doi:10.1016/j.jsg.2012.09.017, 2013.
- 937 Díez Fernández, R., Arenas, R., Pereira, M. F., Sánchez-Martínez, S., Albert, R., Martín Parra,
938 L.-M., Rubio Pascual, F.-J. and Matas, J.: Tectonic evolution of Variscan Iberia: Gondwana–
939 Laurussia collision revisited, *Earth-Sci. Rev.*, 162, 269–292,
940 doi:10.1016/j.earscirev.2016.08.002, 2016.
- 941 Díez-Montes, A.: La Geología del Dominio “Ollo de Sapo” en las comarcas de Sanabria y
942 Terra do Bolo., 2006.
- 943 Díez-Montes, A., Martínez-Catalán, J. R. R. and Bellido-Mulas, F.: Role of the Ollo de Sapo
944 massive felsic volcanism of NW Iberia in the Early Ordovician dynamics of northern Gondwana,
945 *Gondwana Res.*, 17(2–3), 363–376, doi:10.1016/j.gr.2009.09.001, 2010.
- 946 Domeier, M. and Torsvik, T. H.: Plate tectonics in the late Paleozoic, *Geosci. Front.*, 5(3), 303–
947 350, doi:10.1016/j.gsf.2014.01.002, 2014.
- 948 Edel, J. B., Schulmann, K., Lexa, O. and Lardeaux, J. M.: Late Palaeozoic palaeomagnetic and
949 tectonic constraints for amalgamation of Pangea supercontinent in the European Variscan belt,
950 *Earth-Sci. Rev.*, 177(September 2017), 589–612, doi:10.1016/j.earscirev.2017.12.007, 2018.
- 951 Eduard Suess: *Das Antlitz der Erde*, F. Tempsky; [etc., etc.]. [online] Available from:
952 <http://archive.org/details/dasantlitzderer02suesgoog> (Accessed 12 March 2020), 1892.
- 953 Eichelberger, N. and McQuarrie, N.: Kinematic reconstruction of the Bolivian orocline,
954 *Geosphere*, 11(2), 445–462, doi:10.1130/GES01064.1, 2015.
- 955 Escuder Viruete, J., Arenas, R. and Catalán, J. R. M.: Tectonothermal evolution associated with
956 Variscan crustal extension in the Tormes Gneiss Dome (NW Salamanca, Iberian Massif, Spain),
957 *Tectonophysics*, 238(1), 117–138, doi:10.1016/0040-1951(94)90052-3, 1994.
- 958 Fernández-Lozano, J., Pastor-Galán, D., Gutiérrez-Alonso, G. and Franco, P.: New kinematic
959 constraints on the Cantabrian orocline: A paleomagnetic study from the Peñalba and Truchas
960 synclines, NW Spain, *Tectonophysics*, 681, 195–208, doi:10.1016/j.tecto.2016.02.019, 2016.

- 961 Fernández-Lozano, J., Gutiérrez-Alonso, G., Willingshofer, E., Sokoutis, D., Vicente, G. de and
 962 Cloetingh, S.: Shaping of intraplate mountain patterns: The Cantabrian orocline legacy in Alpine
 963 Iberia, *Lithosphere*, 11(5), 708–721, doi:10.1130/L1079.1, 2019.
- 964 Fernández-Suárez, J., Gutiérrez-Alonso, G., Pastor-Galán, D., Hofmann, M., Murphy, J. B. and
 965 Linnemann, U.: The Ediacaran-Early Cambrian detrital zircon record of NW Iberia: Possible
 966 sources and paleogeographic constraints, *Int. J. Earth Sci.*, 103(5), 1335–1357,
 967 doi:10.1007/s00531-013-0923-3, 2014.
- 968 Fossen, H.: *Structural Geology*, Cambridge University Press., 2016.
- 969 Franke, W., Cocks, L. R. M. and Torsvik, T. H.: The Palaeozoic Variscan oceans revisited,
 970 *Gondwana Res.*, 48, 257–284, doi:10.1016/j.jgr.2017.03.005, 2017.
- 971 Franke, W., Cocks, L. R. M. and Torsvik, T. H.: Detrital zircons and the interpretation of
 972 palaeogeography, with the Variscan Orogeny as an example, *Geol. Mag.*, 157(4), 690–694,
 973 doi:10.1017/S0016756819000943, 2020.
- 974 García-Arias, M., Díez-Montes, A., Villaseca, C. and Blanco-Quintero, I. F.: The Cambro-
 975 Ordovician Ollo de Sapo magmatism in the Iberian Massif and its Variscan evolution: A review,
 976 *Earth-Sci. Rev.*, 176, 345–372, doi:10.1016/j.earscirev.2017.11.004, 2018.
- 977 Gil Toja, A., Jimenez-Ontiveros, P., and Seara Valero, J.R., La cuarta fase de deformación
 978 hercinica en la Zona Centroibérica del Macizo Hespérico: Cuadernos Del Laboratorio Xeoloxico
 979 De Laxe, v. 9, p. 91–104, 1985.
- 980 Gong, Z., Langereis, C. G. and Mullender, T. A. T.: The rotation of Iberia during the Aptian and
 981 the opening of the Bay of Biscay, *Earth Planet. Sci. Lett.*, 273(1–2), 80–93, 2008.
- 982 Gozalo, R., Liñán, E., Vintaned, J. A. G., Eugenia, M., Álvarez, D., Martorell, J. B. C., Zamora,
 983 S., Esteve, J. and Mayoral, E.: The Cambrian of the Cadenas Ibéricas (ne Spain) and Its
 984 Trilobites., n.d.
- 985 Greco, K. D., Johnston, S. T., Gutiérrez-Alonso, G., Shaw, J. and Lozano, J. F.: Interference
 986 folding and orocline implications: A structural study of the Ponga Unit, Cantabrian orocline,
 987 northern Spain, *Lithosphere*, 8(6), 757–768, doi:10.1130/L576.1, 2016.
- 988 Gutiérrez Alonso, G.: *Estratigrafía y Tectónica.*, in Memoria del Mapa Geológico de España
 989 1:50000, Hoja de Mora (680), IGME, Madrid. [online] Available from:
 990 <http://info.igme.es/cartografiadigital/datos/magna50/memorias/MMagna0658.pdf>, 2009.
- 991 Gutiérrez-Alonso, G.: El Antiforme del Narcea y su relación con los mantos occidentales de la
 992 Zona Cantábrica., 1992.
- 993 Gutiérrez-Alonso, G.: Strain partitioning in the footwall of the Somiedo Nappe: Structural
 994 evolution of the Narcea Tectonic window, NW Spain, *J. Struct. Geol.*, 18(10), 1217–1229, 1996.
- 995 Gutiérrez-Alonso, G., Fernández-Suárez, J. and Weil, A. B.: Orocline triggered lithospheric
 996 delamination, in Special Paper 383: Orogenic curvature: Integrating paleomagnetic and
 997 structural analyses, vol. 383, edited by A. B. Weil and A. Sussman, pp. 121–130, Geological
 998 Society of America, Boulder., 2004.

- 999 Gutiérrez-Alonso, G., Fernández-Suárez, J., Weil, A. B., Brendan Murphy, J., Damian Nance,
1000 R., Corf, F. and Johnston, S. T.: Self-subduction of the Pangaeon global plate, *Nat. Geosci.*,
1001 1(8), 549–553, doi:10.1038/ngeo250, 2008a.
- 1002 Gutiérrez-Alonso, G., Murphy, J. B. B., Fernández-Suárez, J. and Hamilton, M. A. A.: Rifting
1003 along the northern Gondwana margin and the evolution of the Rheic Ocean: A Devonian age for
1004 the El Castillo volcanic rocks (Salamanca, Central Iberian Zone), *Tectonophysics*, 461(1–4),
1005 157–165, doi:10.1016/j.tecto.2008.01.013, 2008b.
- 1006 Gutiérrez-Alonso, G., Fernández-Suárez, J., Jeffries, T. E. T. E. E., Johnston, S. T., Pastor-
1007 Galán, D., Murphy, J. B. B., Franco, M. P. P., Gonzalo, J. C. C.: Diachronous post-orogenic
1008 magmatism within a developing orocline in Iberia, *European Variscides*, *Tectonics*, 30(5), 17
1009 PP.-17 PP., doi:10.1029/2010TC002845, 2011a.
- 1010 Gutiérrez-Alonso, G., Murphy, J. B., Fernández-Suárez, J., Weil, A. B., Franco, M. P., Gonzalo,
1011 J. C.: Lithospheric delamination in the core of Pangea: Sm-Nd insights from the Iberian mantle,
1012 *Geology*, 39(2), 155–158, doi:10.1130/G31468.1, 2011b.
- 1013 Gutiérrez-Alonso, G., Collins, A. S., Fernández-Suárez, J., Pastor-Galán, D., González-Clavijo,
1014 E., Jourdan, F., Weil, A. B. and Johnston, S. T.: Dating of lithospheric buckling: ⁴⁰Ar/³⁹Ar ages
1015 of syn-orocline strike-slip shear zones in northwestern Iberia, *Tectonophysics*, 643, 44–54,
1016 doi:10.1016/j.tecto.2014.12.009, 2015.
- 1017 Gutiérrez-Alonso, López-Carmona, A., Núñez-Guerrero, E., Martínez García, A., Fernández-
1018 Suárez, J., Pastor-Galán, D., Gutiérrez-Marco, J. C., Bernárdez, E., Colmenero, J. R., Hofmann,
1019 M., Linnemann, U., Neoproterozoic-Palaeozoic detrital sources in the Variscan foreland of
1020 northern Iberia: primary vs. recycled sediments. Pannotia to Pangaea: Neoproterozoic and
1021 Paleozoic Orogenic Cycles in the Circum- Atlantic Region. Accepted in *Geological Society of
1022 London Special Publications*.
- 1023 Gutiérrez-Alonso, G., Fernández-Suárez, J., López-Carmona, A. and Gärtner, A.: Exhuming a
1024 cold case: The early granodiorites of the northwest Iberian Variscan belt—A Visean magmatic
1025 flare-up?, *Lithosphere*, 10(2), 194–216, doi:10.1130/L706.1, 2018.
- 1026 Gutiérrez-Marco, J. C., Sá, A. A., García-Bellido, D. C. and Rábano, I.: The Bohemo-Iberian
1027 regional chronostratigraphical scale for the Ordovician System and palaeontological correlations
1028 within South Gondwana, *Lethaia*, 50(2), 258–295, doi:10.1111/let.12197, 2017.
- 1029 Gutiérrez-Marco, J. C., Piçarra, J. M., Meireles, C. A., Cózar, P., García-Bellido, D. C., Pereira,
1030 Z., Vaz, N., Pereira, S., Lopes, G., Oliveira, J. T., Quesada, C., Zamora, S., Esteve, J.,
1031 Colmenar, J., Bernárdez, E., Coronado, I., Lorenzo, S., Sá, A. A., Dias da Silva, Í., González-
1032 Clavijo, E., Díez-Montes, A. and Gómez-Barreiro, J.: Early Ordovician–Devonian Passive
1033 Margin Stage in the Gondwanan Units of the Iberian Massif, in *The Geology of Iberia: A
1034 Geodynamic Approach*, edited by C. Quesada and J. T. Oliveira, pp. 75–98, Springer
1035 International Publishing, Cham., 2019. Crespo-Blanc, A. and Orozco, M.: The Southern Iberian
1036 Shear Zone: a major boundary in the Hercynian folded belt. *Tectonophysics*, 148(3-4), pp.221-
1037 227., 1988.
- 1038 Hindle, D., Besson, O. and Burkhard, M.: A model of displacement and strain for arc-shaped
1039 mountain belts applied to the Jura arc, *J. Struct. Geol.*, 22(9), 1285–1296, doi:10.1016/S0191-
1040 8141(00)00038-9, 2000.

- 1041 van Hinsbergen, D. J. J., Torsvik, T. H., Schmid, S. M., Mañenco, L. C., Maffione, M., Vissers, R.
1042 L. M., Gürer, D. and Spakman, W.: Orogenic architecture of the Mediterranean region and
1043 kinematic reconstruction of its tectonic evolution since the Triassic, *Gondwana Res.*, 81, 79–
1044 229, doi:10.1016/j.gr.2019.07.009, 2020.
- 1045 Hirt, A. M., Lowrie, W., Julivert, M., Arboleya, M. L., Lowric, A. M. H. W. and Arboleya, M. L.:
1046 Paleomagnetic results in support of a model for the origin of the Asturian arc, *Tectonophysics*,
1047 213(3–4), 321–339, 1992.
- 1048 Hnat, J. S. and van der Pluijm, B. A.: Foreland signature of indenter tectonics: Insights from
1049 calcite twinning analysis in the Tennessee salient of the Southern Appalachians, USA,
1050 *Lithosphere*, 3(5), 317–327, doi:10.1130/L151.1, 2011.
- 1051 Holmes, A.: A review of the continental drift hypothesis., *Min. Mag.*, 40, 205–209, 1929.
- 1052 Huang, W., Lippert, P. C., Zhang, Y., Jackson, M. J., Dekkers, M. J., Li, J., Hu, X., Zhang, B.,
1053 Guo, Z. and van Hinsbergen, D. J. J. J.: Remagnetization of carbonate rocks in southern Tibet:
1054 Perspectives from rock magnetic and petrographic investigations, *J. Geophys. Res. Solid Earth*,
1055 122(4), 2434–2456, doi:10.1002/2017JB013987, 2017.
- 1056 Izquierdo-Llavall, E., Sainz, A. C., Oliva-Urcia, B., Burmester, R., Pueyo, E. L. and Housen, B.:
1057 Multi-episodic remagnetization related to deformation in the Pyrenean Internal Sierras,
1058 *Geophys. J. Int.*, 201(2), 891–914, doi:10.1093/gji/ggv042, 2015.
- 1059 Izquierdo-Llavall, E., Casas-Sainz, A. M., Oliva-Urcia, B., Villalaín, J. J., Pueyo, E. and
1060 Scholger, R.: Rotational Kinematics of Basement Antiformal Stacks: Paleomagnetic Study of the
1061 Western Nogueras Zone (Central Pyrenees), *Tectonics*, 37(10), 3456–3478,
1062 doi:10.1029/2018TC005153, 2018.
- 1063 Izquierdo-Llavall, E., Ayala, C., Pueyo, E. L., Casas-Sainz, A. M., Oliva-Urcia, B., Rubio, F.,
1064 Rodríguez-Pintó, A., Rey-Moral, C., Mediato, J. F. and García-Crespo, J.: Basement-Cover
1065 Relationships and Their Along-Strike Changes in the Linking Zone (Iberian Range, Spain): A
1066 Combined Structural and Gravimetric Study, *Tectonics*, 38(8), 2934–2960,
1067 doi:10.1029/2018TC005422, 2019.
- 1068 Jabaloy-Sánchez, A., Talavera, C., Gómez-Pugnaire, M. T., López-Sánchez-Vizcaíno, V.,
1069 Vázquez-Vílchez, M., Rodríguez-Peces, M. J. and Evans, N. J.: U-Pb ages of detrital zircons
1070 from the Internal Betics: A key to deciphering paleogeographic provenance and tectono-
1071 stratigraphic evolution, *Lithos*, 318–319, 244–266, doi:10.1016/j.lithos.2018.07.026, 2018.
- 1072 Jackson, M.: Diagenetic sources of stable remanence in remagnetized paleozoic cratonic
1073 carbonates: A rock magnetic study, *J. Geophys. Res. Solid Earth*, 95(B3), 2753–2761,
1074 doi:10.1029/JB095iB03p02753, 1990.
- 1075 Jacques, D., Muchez, P. and Sintubin, M.: Superimposed folding and W-Sn vein-type
1076 mineralisation in the Central Iberian Zone associated with late-Variscan oroclinal buckling: A
1077 structural analysis from the Regoufe area (Portugal), *Tectonophysics*, 742–743, 66–83,
1078 doi:10.1016/j.tecto.2018.05.021, 2018a.
- 1079 Jacques, D., Vieira, R., Muchez, P. and Sintubin, M.: Transpressional folding and associated
1080 cross-fold jointing controlling the geometry of post-orogenic vein-type W-Sn mineralization:

- 1081 examples from Minas da Panasqueira, Portugal, *Miner. Deposita*, 53(2), 171–194,
1082 doi:10.1007/s00126-017-0728-6, 2018b.
- 1083 Johnston, S. T.: The Great Alaskan Terrane Wreck: Reconciliation of paleomagnetic and
1084 geological data in the Northern Cordillera, *Earth Planet. Sci. Lett.*, 193(3–4), 259–272,
1085 doi:10.1016/S0012-821X(01)00516-7, 2001.
- 1086 Johnston, S. T., Weil, A. B. and Gutiérrez-Alonso, G.: Oroclines: Thick and thin, *GSA Bull.*,
1087 125(5–6), 643–663, doi:10.1130/B30765.1, 2013.
- 1088 Julivert, M.: *L'évolution structurale de l'Arc Asturien*, Paris., 1971.
- 1089 Julivert, M. and Arboleya, M. L.: A geometrical and kinematical approach to the nappe structure
1090 in an arcuate fold belt: the Cantabrian nappes (Hercynian chain, NW Spain), *J. Struct. Geol.*,
1091 6(5), 499–519, doi:10.1016/0191-8141(84)90061-0, 1984.
- 1092 Julivert, M. and Marcos, A.: superimposed folding under flexural conditions in the Cantabrian
1093 Zone (Hercynian Cordillera, Northwest Spain), *Am. J. Sci.*, 273(5), 353–375,
1094 doi:10.2475/ajs.273.5.353, 1973.
- 1095 Julivert, M., Fontboté, J. M., Ribeiro, A. and Nabais Conde, L. E.: Mapa Tectónico de la
1096 Península Ibérica y Baleares E: 1: 1.000. 000 y memoria explicativa, *Publ IGME*, 113, 1974.
- 1097 Julivert, M., Vegas, R., Roiz, J. M. and Martínez Rius, A.: La estructura de la extensión SE de la
1098 Zona Centro-Iberica con metamorfismo de bajo grado, *Rios-Geol. Esp. I*, 339–380, 1983.
- 1099 Keppie, F.: How subduction broke up Pangaea with implications for the supercontinent cycle,
1100 *Geol. Soc. Lond. Spec. Publ.*, 424(1), 265–288, doi:10.1144/SP424.8, 2016.
- 1101 Kirsch, M., Keppie, J. D., Murphy, J. B. and Solari, L. A.: Permian-Carboniferous arc
1102 magmatism and basin evolution along the western margin of Pangea: Geochemical and
1103 geochronological evidence from the eastern Acatlan Complex, southern Mexico, *Geol. Soc. Am.*
1104 *Bull.*, 124(9–10), 1607–1628, doi:10.1130/B30649.1, 2012.
- 1105 Kollmeier, J. M., van der Pluijm, B. A. and Van der Voo, R.: Analysis of Variscan dynamics;
1106 early bending of the Cantabria-Asturias Arc, northern Spain, *Earth Planet. Sci. Lett.*, 181(1–2),
1107 203–216, doi:10.1016/S0012-821X(00)00203-X, 2000.
- 1108 Kroner, U. and Romer, R. L. L.: Two plates — Many subduction zones: The Variscan orogeny
1109 reconsidered, *Gondwana Res.*, 24(1), 298–329, doi:10.1016/j.gr.2013.03.001, 2013.
- 1110 Leite Mendes, Bruno D., Daniel Pastor-Galán, Mark Dekkers, and Wout Krijgsman. “Avalonia,
1111 Get Bent! Paleomagnetism from SW Iberia Confirms the Greater Cantabrian Orocline.”
1112 Accepted in *Geoscience Frontiers* without DOI yet, Available at EarthArXiv. doi:10.31223/osf.io/
1113 evwc6.
- 1114 Li, P. and Rosenbaum, G.: Does the Manning Orocline exist? New structural evidence from the
1115 inner hinge of the Manning Orocline (eastern Australia), *Gondwana Res.*, 25(4), 1599–1613,
1116 doi:10.1016/j.gr.2013.06.010, 2014.
- 1117 Li, P., Sun, M., Rosenbaum, G., Yuan, C., Safonova, I., Cai, K., Jiang, Y. and Zhang, Y.:

- 1118 Geometry, kinematics and tectonic models of the Kazakhstan Orocline, Central Asian Orogenic
1119 Belt, *J. Asian Earth Sci.*, 153(July 2017), 42–56, doi:10.1016/j.jseae.2017.07.029, 2018.
- 1120 Li, P.-F., Rosenbaum, G. and Rubatto, D.: Triassic asymmetric subduction rollback in the
1121 southern New England Orogen (eastern Australia): the end of the Hunter-Bowen Orogeny, *Aust.*
1122 *J. Earth Sci.*, 59(6), 965–981, doi:10.1080/08120099.2012.696556, 2012.
- 1123 López-Carmona, A., Abati, J., Pitra, P. and Lee, J. K. W.: Retrogressed lawsonite blueschists
1124 from the NW Iberian Massif: P–T–t constraints from thermodynamic modelling and ⁴⁰Ar/³⁹Ar
1125 geochronology, *Contrib. Mineral. Petrol.*, 167(3), 987–987, doi:10.1007/s00410-014-0987-5,
1126 2014.
- 1127 López-Moro, F. J., López-Plaza, M., Gutiérrez-Alonso, G., Fernández-Suárez, J., López-
1128 Carmona, A., Hofmann, M. and Romer, R. L.: Crustal melting and recycling: geochronology and
1129 sources of Variscan syn-kinematic anatectic granitoids of the Tormes Dome (Central Iberian
1130 Zone). A U–Pb LA-ICP-MS study, *Int. J. Earth Sci.*, 107(3), 985–1004, doi:10.1007/s00531-017-
1131 1483-8, 2018.
- 1132 Lotze, F.: Zur gliederung der Variszichen der Iberischen Meseta., *Geotektonische Forschungen*,
1133 6, 78–92, 1945.
- 1134 Macaya, J., González-Lodeiro, F., Martínez-Catalán, J. R. and Alvarez, F.: Continuous
1135 deformation, ductile thrusting and backfolding of cover and basement in the Sierra de
1136 Guadarrama, Hercynian orogen of central Spain, *Tectonophysics*, 191(3), 291–309,
1137 doi:10.1016/0040-1951(91)90063-X, 1991.
- 1138 Maffione, M., Speranza, F. and Faccenna, C.: Bending of the Bolivian orocline and growth of the
1139 central Andean plateau: Paleomagnetic and structural constraints from the Eastern Cordillera
1140 (22–24°S, NW Argentina), *Tectonics*, 28, 23 PP.-23 PP., doi:10.1029/2008TC002402, 2009.
- 1141 Marcos, A. and Pulgar, J. A. A.: An Approach to the tectonostratigraphic evolution of the
1142 Cantabrian foreland thrust and fold belt, Hercynian Cordillera of NW Spain, *Neues Jahrb. Geol.*
1143 *Palaontologie-Abh.*, 163(2), 256–260, 1982.
- 1144 Marcos, A., Pérez-Estaún, A., Martínez Catalán, J. R. and Gutiérrez-Marco, J. C.: *Estratigrafía y*
1145 *Paleogeografía. Zona Asturoccidental-Leonesa*, 2004.
- 1146 Marshak, S.: KINEMATICS OF OROCLINE AND ARC FORMATION IN THIN-SKINNED
1147 OROGENS, *Tectonics*, 7(1), 73–86, 1988.
- 1148 Marshak, S.: Salients, Recesses, Arcs, Oroclines, and Syntaxes — A Review of Ideas
1149 Concerning the Formation of Map-view Curves in Fold-thrust Belts, *Thrust Tecton. Hydrocarb.*
1150 *Syst. AAPG Mem.* 82, 82(1893), 131–156, 2004.
- 1151 Martín-Algarra, A., García-Casco, A., Gómez-Pugnaire, M. T., Jabaloy-Sánchez, A., Laborda-
1152 López, C., López Sánchez-Vizcaíno, V., Mazzoli, S., Navas-Parejo, P., Perrone, V., Rodríguez-
1153 Cañero, R. and Sánchez-Navas, A.: Paleozoic Basement and Pre-Alpine History of the Betic
1154 Cordillera, in *The Geology of Iberia: A Geodynamic Approach*, edited by C. Quesada and J. T.
1155 Oliveira, pp. 261–305, Springer International Publishing, Cham., 2019.
- 1156 Martínez Catalán, J. R.: Are the oroclines of the Variscan belt related to late Variscan strike-slip

- 1157 tectonics?, *Terra Nova*, 23(4), 241–247, doi:10.1111/j.1365-3121.2011.01005.x, 2011.
- 1158 Martínez Catalán, J. R.: The Central Iberian arc, an orocline centered in the Iberian Massif and
1159 some implications for the Variscan belt, *Int. J. Earth Sci.*, 101(5), 1–16, doi:10.1007/s00531-
1160 011-0715-6, 2012.
- 1161 Martínez Catalan, J. R., Rodríguez, M. P. H., Alonso, P. V., Perez-Estaun, A. and Lodeiro, F. G.:
1162 Lower Paleozoic extensional tectonics in the limit between the West Asturian-Leonese and
1163 Central Iberian Zones of the Variscan Fold-Belt in NW Spain, *Geol. Rundsch.*, 81(2), 545–560,
1164 doi:10.1007/BF01828614, 1992.
- 1165 Martínez Catalán, J. R., Martínez Poyatos, D. and Bea, F.: Zona Centroibérica, *Geol. Esp.*, 68–
1166 133, 2004.
- 1167 Martínez-Catalán, J. R. M., Fernández-Suárez, J., Jenner, G. A., Belousova, E. and Montes, A.:
1168 Provenance constraints from detrital zircon U–Pb ages in the NW Iberian Massif: implications
1169 for Palaeozoic plate configuration and Variscan evolution, *J. Geol. Soc.*, 161(3), 463–476,
1170 doi:10.1144/0016-764903-054, 2004.
- 1171 Martínez Catalán, J. R., Arenas, R., Abati, J., Martínez, S. S., García, F. D., Suárez, J. F.,
1172 Cuadra, P. G., Castiñeiras, P., Barreiro, J. G., Montes, A. D., Clavijo, E. G., Pascual, F. J. R.,
1173 Andonaegui, P., Jeffries, T. E., Alcock, J. E., Fernández, R. D. and Carmona, A. L.: A rootless
1174 suture and the loss of the roots of a mountain chain: The Variscan belt of NW Iberia, *Comptes
1175 Rendus Geosci.*, 341(2), 114–126, doi:10.1016/j.crte.2008.11.004, 2009.
- 1176 Martínez Catalan, J. R., Rubio Pascual, F. J., Díez Montes, A., Díez Fernández, R., Gómez
1177 Barreiro, J., Dias da Silva, I., González Clavijo, E., Ayarza, P., Alcock, J. E.: The late Variscan
1178 HT/LP metamorphic event in NW and Central Iberia: relationships to crustal thickening,
1179 extension, orocline development and crustal evolution, *Geol. Soc. Lond. Spec. Publ.*, 405(1),
1180 225–247, doi:10.1144/SP405.1, 2014.
- 1181 Martínez Catalán, J. R., Aerden, D. G. A. M. and Carreras, J.: The “Castilian bend” of Rudolf
1182 Staub (1926): historical perspective of a forgotten orocline in Central Iberia, *Swiss J. Geosci.*,
1183 108(2–3), 289–303, doi:10.1007/s00015-015-0202-3, 2015.
- 1184 Martínez Catalán, J. R., Gómez Barreiro, J., Dias da Silva, Í., Chichorro, M., López-Carmona,
1185 A., Castiñeiras, P., Abati, J., Andonaegui, P., Fernández-Suárez, J., González Cuadra, P. and
1186 Benítez-Pérez, J. M.: Variscan Suture Zone and Suspect Terranes in the NW Iberian Massif:
1187 Allochthonous Complexes of the Galicia-Trás os Montes Zone (NW Iberia), in *The Geology of
1188 Iberia: A Geodynamic Approach*, edited by C. Quesada and J. T. Oliveira, pp. 99–130, Springer
1189 International Publishing, Cham., 2019.
- 1190 Martínez-Catalán, J. R.: A non-cylindrical model for the northwest Iberian allochthonous
1191 terranes and their equivalents in the Hercynian belt of Western Europe, *Tectonophysics*, 179(3–
1192 4), 253–272, doi:10.1016/0040-1951(90)90293-H, 1990.
- 1193 McWilliams, C. K., Kunk, M. J., Wintsch, R. P. and Bish, D. L.: Determining ages of multiple
1194 muscovite-bearing foliations in phyllonites using the $^{40}\text{Ar}/^{39}\text{Ar}$ step heating method:
1195 Applications to the alleghanian orogeny in central new England, *Am. J. Sci.*, 313(10), 996–1016,
1196 doi:10.2475/10.2013.02, 2013.

- 1197 Meijers, M. J. M., Smith, B., Pastor-Galán, D., Degenaar, R., Sadradze, N., Adamia, S.,
 1198 Sahakyan, L., Avagyan, A., Sosson, M., Rolland, Y., Langereis, C. G. and Müller, C.:
 1199 Progressive orocline formation in the Eastern Pontides-Lesser Caucasus, *Geol. Soc. Spec.*
 1200 *Publ.*, 428(1), doi:10.1144/SP428.8, 2017.
- 1201 Merino-Tomé, O. A., Bahamonde, J. R., Colmenero, J. R., Heredia, N., Villa, E. and Farias, P.:
 1202 Emplacement of the Cuera and Picos de Europa imbricate system at the core of the Iberian-
 1203 Armorican arc (Cantabrian zone, north Spain): New precisions concerning the timing of arc
 1204 closure, *Bull. Geol. Soc. Am.*, 121(5–6), 729–751, doi:10.1130/B26366.1, 2009.
- 1205 Molina Garza, R. S. and Zijdeveld, J. D. a.: Paleomagnetism of Paleozoic strata, Brabant and
 1206 Ardennes Massifs, Belgium: Implications of prefolding and postfolding Late Carboniferous
 1207 secondary magnetizations for European apparent polar wander, *J. Geophys. Res.*, 101(B7),
 1208 15799–15799, doi:10.1029/96JB00325, 1996.
- 1209 Moral, B. del and Sarmiento, G. N.: Conodontos del Katiense (Ordovícico Superior) del sector
 1210 meridional de la Zona Centroibérica (España), *Rev. Esp. Micropaleontol.*, 40(3), 169–245, 2008.
- 1211 Munha, J.: Metamorphic Evolution of the South Portuguese/Pulo Do Lobo Zone, in *Pre-*
 1212 *Mesozoic Geology of Iberia*, edited by R. D. Dallmeyer and E. M. Garcia, pp. 363–368,
 1213 Springer, Berlin, Heidelberg., 1990.
- 1214 Munha, J., Barriga, F. J. a. S. and Kerrich, R.: High 18 O ore-forming fluids in volcanic-hosted
 1215 base metal massive sulfide deposits; geologic, 18 O/ 16 O, and D/H evidence from the Iberian
 1216 pyrite belt; Crandon, Wisconsin; and Blue Hill, Maine, *Econ. Geol.*, 81(3), 530–552, doi:10.2113/
 1217 gsecongeo.81.3.530, 1986.
- 1218 Murphy, J. B., Gutierrez-Alonso, G., Fernandez-Suarez, J. and Braid, J. A.: Probing crustal and
 1219 mantle lithosphere origin through Ordovician volcanic rocks along the Iberian passive margin of
 1220 Gondwana, *Tectonophysics*, 461(1–4), 166–180, 2008.
- 1221 Nance, R. D., Gutiérrez-Alonso, G., Keppie, J. D., Linnemann, U., Murphy, J. B., Quesada, C.,
 1222 Strachan, R. A. and Woodcock, N. H.: Evolution of the Rheic Ocean, *Gondwana Res.*, 17(2–3),
 1223 194–222, doi:10.1016/j.gr.2009.08.001, 2010.
- 1224 Oliveira, J. T., Quesada, C., Pereira, Z., Matos, J. X., Solá, A. R., Rosa, D., Albardeiro, L., Díez-
 1225 Montes, A., Morais, I., Inverno, C., Rosa, C. and Relvas, J.: South Portuguese Terrane: A
 1226 Continental Affinity Exotic Unit, in *The Geology of Iberia: A Geodynamic Approach*, edited by C.
 1227 Quesada and J. T. Oliveira, pp. 173–206, Springer International Publishing, Cham., 2019a.
- 1228 Oliveira, J. T., González-Clavijo, E., Alonso, J., Armendáriz, M., Bahamonde, J. R., Braid, J. A.,
 1229 Colmenero, J. R., Dias da Silva, Í., Fernandes, P., Fernández, L. P., Gabaldón, V., Jorge, R. S.,
 1230 Machado, G., Marcos, A., Merino-Tomé, Ó., Moreira, N., Murphy, J. B., Pinto de Jesus, A.,
 1231 Quesada, C., Rodrigues, B., Rosales, I., Sanz-López, J., Suárez, A., Villa, E., Piçarra, J. M. and
 1232 Pereira, Z.: Synorogenic Basins, in *The Geology of Iberia: A Geodynamic Approach*, edited by
 1233 C. Quesada and J. T. Oliveira, pp. 349–429, Springer International Publishing, Cham., 2019b.
- 1234 P. Farias, G. G.: Aportaciones al conocimiento de la litoestratigrafía y estructura de Galicia
 1235 Central, *Mem. Fac. Ciênc. Universidade Porto*, 411–431, 1987.
- 1236 Palero-Fernández, F. J., Martin-Izard, A., Zorzalejos Prieto, M. and Mansilla-Plaza, L.:

- 1237 Geological context and plumbotectonic evolution of the giant Almadén Mercury Deposit, Ore
1238 Geol. Rev., 64, 71–88, doi:10.1016/j.oregeorev.2014.06.013, 2015.
- 1239 Parés, J. M. and Van der Voo, R.: Paleozoic paleomagnetism of Almaden, Spain: A cautionary
1240 note, J. Geophys. Res., 97(B6), 9353–9356, doi:10.1029/91JB03073, 1992.
- 1241 Parés, J. M., Van der Voo, R., Stamatakos, J. and Pérez–Estaún, A.: Remagnetizations and
1242 postfolding oroclinal rotations in the Cantabrian/Asturian arc, northern Spain, Tectonics, 13(6),
1243 1461–1471, doi:10.1029/94TC01871, 1994.
- 1244 Pastor-Galán, D., Gutiérrez-Alonso, G., Meere, P. A. and Mulchrone, K. F.: Factors affecting
1245 finite strain estimation in low-grade, low-strain clastic rocks, J. Struct. Geol., 31(12), 1586–1596,
1246 doi:10.1016/j.jsg.2009.08.005, 2009.
- 1247 Pastor-Galán, D., Gutiérrez-Alonso, G. and Weil, A. B.: Orocline timing through joint analysis:
1248 Insights from the Ibero-Armorican Arc, Tectonophysics, 507(1), 31–46,
1249 doi:10.1016/j.tecto.2011.05.005, 2011.
- 1250 Pastor-Galán, D., Gutiérrez-Alonso, G., Zulauf, G. and Zanella, F.: Analogue modeling of
1251 lithospheric-scale orocline buckling: Constraints on the evolution of the Iberian-Armorican arc,
1252 Bull. Geol. Soc. Am., 124(7–8), doi:10.1130/B30640.1, 2012a.
- 1253 Pastor-Galán, D., Gutiérrez-Alonso, G., Mulchrone, K. F. and Huerta, P.: Conical folding in the
1254 core of an orocline. A geometric analysis from the Cantabrian Arc (Variscan Belt of NW Iberia),
1255 J. Struct. Geol., 39, 210–223, doi:10.1016/j.jsg.2012.02.010, 2012b.
- 1256 Pastor-Galán, D., Gutiérrez-Alonso, G., Murphy, J. B. B., Fernández-Suárez, J., Hofmann, M.
1257 and Linnemann, U.: Provenance analysis of the Paleozoic sequences of the northern
1258 Gondwana margin in NW Iberia: Passive margin to Variscan collision and orocline development,
1259 Gondwana Res., 23(3), 1089–1103, doi:10.1016/j.gr.2012.06.015, 2013a.
- 1260 Pastor-Galán, D., Gutiérrez-Alonso, G., Fernández-Suárez, J., Murphy, J. B. and Nieto, F.:
1261 Tectonic evolution of NW Iberia during the Paleozoic inferred from the geochemical record of
1262 detrital rocks in the Cantabrian Zone, Lithos, 182–183, 221–228,
1263 doi:10.1016/j.lithos.2013.09.007, 2013b.
- 1264 Pastor-Galán, D., Martín-Merino, G. and Corrochano, D.: Timing and structural evolution in the
1265 limb of an orocline: The Pisuerga-Carrión Unit (southern limb of the Cantabrian Orocline, NW
1266 Spain), Tectonophysics, 622, 110–121, doi:10.1016/j.tecto.2014.03.004, 2014.
- 1267 Pastor-Galán, D., Ursem, B., Meere, P. A. and Langereis, C.: Extending the Cantabrian
1268 Orocline to two continents (from Gondwana to Laurussia). Paleomagnetism from South Ireland,
1269 Earth Planet. Sci. Lett., 432, doi:10.1016/j.epsl.2015.10.019, 2015a.
- 1270 Pastor-Galán, D., Groenewegen, T., Brouwer, D., Krijgsman, W., Dekkers, M. J., Pastor-galán,
1271 D., Groenewegen, T., Brouwer, D., Krijgsman, W. and Dekkers, M. J.: One or two oroclines in
1272 the Variscan orogen of Iberia? Implications for Pangea amalgamation, Geology, 43(6), 527–
1273 530, doi:10.1130/G36701.1, 2015b.
- 1274 Pastor-Galán, D., Dekkers, M. J., Gutiérrez-Alonso, G., Brouwer, D., Groenewegen, T.,
1275 Krijgsman, W., Fernández-Lozano, J., Yenes, M. and Álvarez-Lobato, F.: Paleomagnetism of

- 1276 the Central Iberian curve's putative hinge: Too many oroclines in the Iberian Variscides,
1277 *Gondwana Res.*, 39, 96–113, doi:10.1016/j.gr.2016.06.016, 2016.
- 1278 Pastor-Galán, D., Mulchrone, K. F., Koymans, M. R. , van Hinsbergen, D. J. J. and Langereis,
1279 C. G. : Bootstrapped total least squares orocline test: A robust method to quantify vertical-axis
1280 rotation patterns in orogens, with examples from the Cantabrian and Aegean oroclines,
1281 *Lithosphere*, 9(3), L547.1-L547.1, doi:10.1130/L547.1, 2017a.
- 1282 Pastor-Galán, D., Gutiérrez-Alonso, G., Dekkers, M. J. M. J. and Langereis, C. G.:
1283 Paleomagnetism in Extremadura (Central Iberian zone, Spain) Paleozoic rocks: extensive
1284 remagnetizations and further constraints on the extent of the Cantabrian orocline, *J. Iber. Geol.*,
1285 43(4), 583–600, doi:10.1007/s41513-017-0039-x, 2017b.
- 1286 Pastor-Galán, D., Pueyo, E. L., Diederer, M., García-Lasanta, C. and Langereis, C. G.: Late
1287 Paleozoic Iberian Orocline(s) and the Missing Shortening in the Core of Pangea.
1288 Paleomagnetism From the Iberian Range, *Tectonics*, 37(10), 3877–3892,
1289 doi:10.1029/2018TC004978, 2018.
- 1290 Pastor-Galán, D., Nance, R. D., Murphy, J. B. and Spencer, C. J.: Supercontinents: myths,
1291 mysteries, and milestones, *Geol. Soc. Lond. Spec. Publ.*, 470, 39–64, doi:10.1144/SP470.16,
1292 2019a.
- 1293 Pastor-Galán, D., Dias da Silva, Í. F., Groenewegen, T. and Krijgsman, W.: Tangled up in folds:
1294 tectonic significance of superimposed folding at the core of the Central Iberian curve (West
1295 Iberia), *Int. Geol. Rev.*, 61(2), 240–255, doi:10.1080/00206814.2017.1422443, 2019b.
- 1296 Pereira, I., Dias, R., Bento, T. and Mata, J.: Exhumation of a migmatite complex along a
1297 transpressive shear zone : inferences from the Variscan Juzbado – Penalva do Castelo Shear
1298 Zone (Central Iberian Zone), *J. Geol. Soc.*, doi:10.1144/jgs2016-159, 2017.
- 1299 Pereira, M. F., Chichorro, M., Silva, J. B., Ordóñez-Casado, B., Lee, J. K. W. W. and Williams, I.
1300 S.: Early carboniferous wrenching, exhumation of high-grade metamorphic rocks and basin
1301 instability in SW Iberia: Constraints derived from structural geology and U–Pb and 40Ar–39Ar
1302 geochronology, *Tectonophysics*, 558, 28–44, doi:10.1016/j.tecto.2012.06.020, 2012.
- 1303 Pereira, M. F., Díez Fernández, R., Gama, C., Hofmann, M., Gärtner, A. and Linnemann, U.: S-
1304 type granite generation and emplacement during a regional switch from extensional to
1305 contractional deformation (Central Iberian Zone, Iberian autochthonous domain, Variscan
1306 Orogeny), *Int. J. Earth Sci.*, 107(1), 251–267, doi:10.1007/s00531-017-1488-3, 2018.
- 1307 Pérez-Cáceres, I., Poyatos, D. M., Simancas, J. F. and Azor, A.: The elusive nature of the
1308 Rheic Ocean suture in SW Iberia, *Tectonics*, 34(12), 2429–2450, doi:10.1002/2015TC003947,
1309 2015.
- 1310 Pérez-Cáceres, I., Simancas, J. F., Martínez Poyatos, D., Azor, A. and González Lodeiro, F.:
1311 Oblique collision and deformation partitioning in the SW Iberian Variscides, *Solid Earth*, 7(3),
1312 857–872, doi:https://doi.org/10.5194/se-7-857-2016, 2016.
- 1313 Pérez-Cáceres, I., Martínez Poyatos, D., Simancas, J. F. and Azor, A.: Testing the Avalonian
1314 affinity of the South Portuguese Zone and the Neoproterozoic evolution of SW Iberia through
1315 detrital zircon populations, *Gondwana Res.*, 42, 177–192, doi:10.1016/j.gr.2016.10.010, 2017.

- 1316 Pérez-Cáceres, I., Martínez Poyatos, D. J., Vidal, O., Beyssac, O., Nieto, F., Simancas, J. F.,
 1317 Azor, A. and Bourdelle, F.: Deciphering the metamorphic evolution of the Pulo do Lobo
 1318 metasedimentary domain (SW Iberian Variscides), *Solid Earth*, 11(2), 469–488,
 1319 doi:<https://doi.org/10.5194/se-11-469-2020>, 2020.
- 1320 Pérez-Estaún, A., Bastida, F., Alonso, J. L., Marquinez, J., Aller, J., Alvarezmarron, J., Marcos,
 1321 A. and Pulgar, J. A.: A THIN-SKINNED TECTONICS MODEL FOR AN ARCUATE FOLD AND
 1322 THRUST BELT - THE CANTABRIAN ZONE (VARISCAN IBERO-ARMORICAN ARC),
 1323 *Tectonics*, 7(3), 517–537, 1988.
- 1324 Pérez-Estaún, A., Bastida, F., Martínez Catalán, J. R., Gutiérrez-Marco, J. C., Marcos, A. and
 1325 Pulgar, J.: *Stratigraphy of the West Asturian-Leonese Zone*, Springer. [online] Available from:
 1326 <https://digital.csic.es/handle/10261/30719> (Accessed 6 April 2020), 1990.
- 1327 Pérez-Estaún, A., Martinezcatalan, J. R. and Bastida, F.: CRUSTAL THICKENING AND
 1328 DEFORMATION SEQUENCE IN THE FOOTWALL TO THE SUTURE OF THE VARISCAN
 1329 BELT OF NORTHWEST SPAIN, *Tectonophysics*, 191(3–4), 243–253, 1991.
- 1330 Perroud, H., Bonhommet, N. and Ribeiro, A.: Paleomagnetism of Late Paleozoic igneous rocks
 1331 from southern Portugal, *Geophys. Res. Lett.*, 12(1), 45–48, doi:10.1029/GL012i001p00045,
 1332 1985.
- 1333 Perroud, H., Calza, F. and Khattach, D.: Paleomagnetism of the Silurian Volcanism at Almaden,
 1334 Southern Spain, *J. Geophys. Res.-Solid Earth Planets*, 96(B2), 1949–1962,
 1335 doi:10.1029/90JB02226, 1991.
- 1336 Pin, C., Paquette, J. L., Zalduegui, J. F. S. and Ibarra, J. I. G.: Early Devonian
 1337 suprasubduction-zone ophiolite related to incipient collisional processes in the Western
 1338 Variscan Belt: The Sierra de Careón unit, Ordenes Complex, Galicia, in *Variscan-Appalachian*
 1339 *dynamics: The building of the late Paleozoic basement*, Geological Society of America., 2002.
- 1340 Pueyo, E. L., Mauritsch, H. J., Gawlick, H.-J., Scholger, R. and Frisch, W.: New evidence for
 1341 block and thrust sheet rotations in the central northern Calcareous Alps deduced from two
 1342 pervasive remagnetization events, *Tectonics*, 26(5), n/a-n/a, doi:10.1029/2006TC001965, 2007.
- 1343 Pueyo, E. L., Sussman, A. J., Oliva-Urcia, B. and Cifelli, F.: Palaeomagnetism in fold and thrust
 1344 belts: Use with caution, *Geol. Soc. Spec. Publ.*, 425(1), 259–276, doi:10.1144/SP425.14, 2016.
- 1345 Quesada, C.: The Ossa-Morena Zone of the Iberian Massif: a tectonostratigraphic approach to
 1346 its evolution, *Z. Dtsch. Ges. Für Geowiss.*, 585–595, doi:10.1127/1860-1804/2006/0157-0585,
 1347 2006.
- 1348 Quesada, C. and Dallmeyer, R. D. D.: Tectonothermal evolution of the Badajoz-Córdoba shear
 1349 zone (SW Iberia): characteristics and ⁴⁰Ar/³⁹Ar mineral age constraints, *Tectonophysics*,
 1350 231(1–3), 195–213, doi:10.1016/0040-1951(94)90130-9, 1994.
- 1351 Quesada, C., Braid, J. A., Fernandes, P., Ferreira, P., Jorge, R. S., Matos, J. X., Murphy, J. B.,
 1352 Oliveira, J. T., Pedro, J. and Pereira, Z.: SW Iberia Variscan Suture Zone: Oceanic Affinity
 1353 Units, in *The Geology of Iberia: A Geodynamic Approach*, edited by C. Quesada and J. T.
 1354 Oliveira, pp. 131–171, Springer International Publishing, Cham., 2019.

- 1355 Rankin, D. W.: Appalachian salients and recesses: Late Precambrian continental breakup and
 1356 the opening of the Iapetus Ocean, *J. Geophys. Res.* 1896-1977, 81(32), 5605–5619,
 1357 doi:10.1029/JB081i032p05605, 1976.
- 1358 Ribeiro, A., Munhá, J., Dias, R., Mateus, A., Pereira, E., Ribeiro, L., Fonseca, P., Araújo, A.,
 1359 Oliveira, T., Romão, J., Chaminé, H., Coke, C. and Pedro, J.: Geodynamic evolution of the SW
 1360 Europe Variscides, *Tectonics*, 26(6), doi:10.1029/2006TC002058, 2007.
- 1361 Ries, A. C. and Shackleton, R. M.: Catazonal Complexes of North-West Spain and North
 1362 Portugal, Remnants of a Hercynian Thrust Plate, *Nat. Phys. Sci.*, 234(47), 65–68,
 1363 doi:10.1038/physci234065a0, 1971.
- 1364 Ries, A. C. and Shackleton, R. M.: Patterns of Strain Variation in Arcuate Fold Belts, *Philos.*
 1365 *Trans. R. Soc. Lond. Ser. Math. Phys. Sci.*, 283(1312), 281–288, 1976.
- 1366 Rodríguez-Cañero, R., Jabaloy-Sánchez, A., Navas-Parejo, P., Martín-Algarra, A., Rodríguez,
 1367 R., Antonio, C., Sánchez, J., Navas, P., Agustín, P. and Algarra, M.: Linking Palaeozoic
 1368 palaeogeography of the Betic Cordillera to the Variscan Iberian Massif : new insight through the
 1369 first conodonts of the Nevado-Filábride Complex, *Int. J. Earth Sci.*, 107(5), 1791–1806,
 1370 doi:10.1007/s00531-017-1572-8, 2018.
- 1371 Rosenbaum, G.: Geodynamics of oroclinal bending: Insights from the Mediterranean, *J.*
 1372 *Geodyn.*, 82, 5–15, doi:10.1016/j.jog.2014.05.002, 2014.
- 1373 Rubio Pascual, F. J., Arenas, R., Martínez Catalán, J. R., Rodríguez Fernández, L. R. and
 1374 Wijbrans, J. R.: Thickening and exhumation of the Variscan roots in the Iberian Central System:
 1375 Tectonothermal processes and $40\text{Ar}/39\text{Ar}$ ages, *Tectonophysics*, 587, 207–221,
 1376 doi:10.1016/j.tecto.2012.10.005, 2013.
- 1377 Rubio Pascual, F. J., López-Carmona, A. and Arenas, R.: Thickening vs. extension in the
 1378 Variscan belt: P–T modelling in the Central Iberian autochthon, *Tectonophysics*, 681, 144–158,
 1379 doi:10.1016/j.tecto.2016.02.033, 2016.
- 1380 Sánchez-García, T., Chichorro, M., Solá, A. R., Álvaro, J. J., Díez-Montes, A., Bellido, F.,
 1381 Ribeiro, M. L., Quesada, C., Lopes, J. C., Dias da Silva, Í., González-Clavijo, E., Gómez
 1382 Barreiro, J. and López-Carmona, A.: The Cambrian-Early Ordovician Rift Stage in the
 1383 Gondwanan Units of the Iberian Massif, in *The Geology of Iberia: A Geodynamic Approach*,
 1384 edited by C. Quesada and J. T. Oliveira, pp. 27–74, Springer International Publishing, Cham.,
 1385 2019.
- 1386 Schulz, G.: Descripción geológica de Asturias: Publicada de Real Órden. Con un atlas, José
 1387 Gonzalez., 1858.
- 1388 Schwartz, S. Y. and Vandervoo, R.: PALEOMAGNETIC EVALUATION OF THE OROCLINE
 1389 HYPOTHESIS IN THE CENTRAL AND SOUTHERN APPALACHIANS, *Geophys. Res. Lett.*,
 1390 10(7), 505–508, 1983.
- 1391 Shaw, J. and Johnston, S. T.: Terrane wrecks (coupled oroclinal) and paleomagnetic inclination
 1392 anomalies, *Earth-Sci. Rev.*, 154, 191–209, doi:10.1016/j.earscirev.2016.01.003, 2016.
- 1393 Shaw, J., Johnston, S. T., Gutiérrez-Alonso, G. and Weil, A. B.: Oroclines of the Variscan

- 1394 orogen of Iberia: Paleocurrent analysis and paleogeographic implications, *Earth Planet. Sci.*
1395 *Lett.*, 329–330, 60–70, doi:10.1016/j.epsl.2012.02.014, 2012.
- 1396 Shaw, J., Johnston, S. T., Gutiérrez-Alonso, G. and Pastor-Galán, D.: Provenance variability
1397 along the Early Ordovician north Gondwana margin: Paleogeographic and tectonic implications
1398 of U-Pb detrital zircon ages from the Armorican Quartzite of the Iberian Variscan belt, *Bull. Geol.*
1399 *Soc. Am.*, 126(5–6), 702–719, doi:10.1130/B30935.1, 2014.
- 1400 Shaw, J., Johnston, S. T. and Gutiérrez-Alonso, G.: Orocline formation at the core of Pangea: A
1401 structural study of the Cantabrian orocline, NW Iberian Massif, *Lithosphere*, 7(6), 653–661,
1402 doi:10.1130/L461.1, 2015.
- 1403 Shaw, J., Johnston, S. T. and Gutiérrez-Alonso, G.: Orocline formation at the core of Pangea: A
1404 structural study of the Cantabrian orocline, NW Iberian Massif, *Lithosphere*, 8(1), 97–97,
1405 doi:10.1130/L461.1, 2016.
- 1406 Silva, Í. D. D., Valverde-Vaquero, P., González-Clavijo, E., Díez-Montes, A. and Catalán, J. R.
1407 M.: Structural and stratigraphical significance of U–Pb ages from the Mora and Saldanha
1408 volcanic complexes (NE Portugal, Iberian Variscides), *Geol. Soc. Lond. Spec. Publ.*, 405(1),
1409 115–135, doi:10.1144/SP405.3, 2014.
- 1410 Simancas, J. F., Carbonell, R., Lodeiro, F. G., Estaun, A., Juhlin, C., Ayarza, P., Kashubin, A.,
1411 Azor, A., Poyatos, D. M., Almodovar, G. R., Pascual, E., Saez, R. and Exposito, I.: Crustal
1412 structure of the transpressional Variscan orogen of SW Iberia: SW Iberia deep seismic reflection
1413 profile (IBERSEIS), *Tectonics*, 22(6), 25–25, 2003.
- 1414 Simancas, J. F., Ayarza, P., Azor, a., Carbonell, R., Martínez Poyatos, D., Pérez-Estaún, a. and
1415 González Lodeiro, F.: A seismic geotraverse across the Iberian Variscides: Orogenic
1416 shortening, collisional magmatism, and orocline development, *Tectonics*, 32(i), n/a-n/a,
1417 doi:10.1002/tect.20035, 2013.
- 1418 Solís-Alulima, B. E., López-Carmona, A., Gutiérrez Alonso, G. and Álvarez Valero, A. M.:
1419 Petrologic and thermobarometric study of the Riás schists (NW Iberian Massif), *Bol. Geológico*
1420 *Min.*, 130(3), 445–464, doi:10.21701/bolgeomin.130.3.004, 2019.
- 1421 Stampfli, G. M. and Borel, G. D.: The TRANSMED Transects in Space and Time: Constraints
1422 from Paleotectonic Evolution of the Mediterranean Domain., edited by W. Cavazza, F. M.
1423 Roure, W. Spakman, G. M. Stampfli, and P. A. Ziegler, pp. 53–80, Springer, Berlin., 2004.
- 1424 Stampfli, G. M., Hochard, C., Vérard, C., Wilhem, C. and VonRaumer, J.: The Formation of
1425 Pangea, *Tectonophysics*, 593, 1–19, doi:10.1016/j.tecto.2013.02.037, 2013.
- 1426 Staub, R.: Gedanken zur Tektonik Spaniens., Zürich., 1926.
- 1427 Stewart, S. A.: Paleomagnetic analysis of fold kinematics and implications for geological models
1428 of the Cantabrian/Asturian arc, north Spain, *J. Geophys. Res. Solid Earth*, 100(B10), 20079–
1429 20094, doi:10.1029/95JB01482, 1995.
- 1430 Tait, J. A., Bachtadse, V. and Soffel, H. C.: Eastern Variscan fold belt : Paleomagnetic evidence
1431 for oroclinal bending, *Geology*, 24, 871–874, doi:10.1130/0091-7613(1996)024<0871, 1996.

- 1432 Tauxe, L.: *Essentials of Paleomagnetism*, Univ of California Press., 2010.
- 1433 Thomas, W. A.: Evolution of Appalachian-Ouachita Salients and Recesses from Reentrants and
1434 Promontories in the Continental Margin, *Am. J. Sci.*, 277(10), 1233–1278,
1435 doi:10.2475/ajs.277.10.1233, 1977.
- 1436 Thomas, W. A.: Genetic relationship of rift-stage crustal structure, terrane accretion, and
1437 foreland tectonics along the southern Appalachian-Ouachita orogen, *J. Geodyn.*, 37(3), 549–
1438 563, doi:10.1016/j.jog.2004.02.020, 2004.
- 1439 Tohver, E., Weil, A. B. B. B., Solum, J. G. G. G. and Hall, C. M. M. M.: Direct dating of
1440 carbonate remagnetization by $^{40}\text{Ar}/^{39}\text{Ar}$ analysis of the smectite–illite transformation, *Earth
1441 Planet. Sci. Lett.*, 274(3–4), 524–530, doi:10.1016/j.epsl.2008.08.002, 2008.
- 1442 Toit, A. L. Du: *Our wandering continents: an hypothesis of continental drifting*, Oliver and Boyd.
1443 [online] Available from: <http://books.google.es/books?id=iDZEAAAIAAJ>, 1937.
- 1444 Valladares, M. I., Barba, P., Ugidos, J. M., Colmenero, J. R. and Armenteros, I.: Upper
1445 Neoproterozoic-Lower Cambrian sedimentary successions in the Central Iberian Zone (Spain):
1446 sequence stratigraphy, petrology and chemostratigraphy. Implications for other European
1447 zones, *Int. J. Earth Sci.*, 89(1), 2–20, 2000.
- 1448 Van der Voo, R.: Paleomagnetism, oroclines, and growth of the continental crust, *GSA Today*,
1449 14(12), 4–9, doi:10.1130/1052-5173(2004), 2004.
- 1450 Vergés, J.: Estudio del Complejo volcánico-sedimentario del Devónico y de la estructura de la
1451 terminación oriental del sinclinal de Almadén (Ciudad Real), in *Libro Jubilar JM Rios. Tomo 3*,
1452 pp. 215–229., 1983.
- 1453 Vissers, R. L. M., van Hinsbergen, D. J. J., van der Meer, D. G. and Spakman, W.: Cretaceous
1454 slab break-off in the Pyrenees: Iberian plate kinematics in paleomagnetic and mantle reference
1455 frames, *Gondwana Res.*, 34, 49–59, doi:10.1016/J.GR.2016.03.006, 2016.
- 1456 van der Voo, R., Stamatakos, J. A. and Pares, J. M.: Kinematic constraints on thrust-belt
1457 curvature from syndeformational magnetizations in the Lagos del Valle Syncline in the
1458 Cantabrian Arc, Spain, *J. Geophys. Res.-Solid Earth*, 102(B5), 10105–10119, 1997.
- 1459 Weil, A., Pastor-Galán, D., Johnston, S. T. and Gutiérrez-Alonso, G.: Late/Post Variscan
1460 Orocline Formation and Widespread Magmatism, in *The Geology of Iberia: A Geodynamic
1461 Approach*, edited by C. Quesada and J. T. Oliveira, pp. 527–542, Springer International
1462 Publishing, Cham., 2019.
- 1463 Weil, A. B.: Kinematics of orocline tightening in the core of an arc: Paleomagnetic analysis of
1464 the Ponga Unit, Cantabrian Arc, northern Spain, *Tectonics*, 25(3), n/a-n/a,
1465 doi:10.1029/2005TC001861, 2006.
- 1466 Weil, A. B. and Sussman, A. J.: Classifying curved orogens based on timing relationships
1467 between structural development and vertical-axis rotations, vol. 383, edited by A. J. Sussman
1468 and A. B. Weil, pp. 1–16, Geological Society of America., 2004.
- 1469 Weil, A. B., Van der Voo, R., van der Pluijm, B. A. and Parés, J. M.: The formation of an orocline

- 1470 by multiphase deformation: a paleomagnetic investigation of the Cantabria–Asturias Arc
1471 (northern Spain), *J. Struct. Geol.*, 22(6), 735–756, doi:10.1016/S0191-8141(99)00188-1, 2000.
- 1472 Weil, A. B., van der Voo, R. and van der Pluijm, B. A.: Oroclinal bending and evidence against
1473 the Pangea megashear: The Cantabria-Asturias arc (northern Spain), *Geology*, 29(11), 991–
1474 994, 2001.
- 1475 Weil, A. B., Van der Voo, R. and Voo, R. V. D.: Insights into the mechanism for orogen-related
1476 carbonate remagnetization from growth of authigenic Fe-oxide: A scanning electron microscopy
1477 and rock magnetic study of Devonian carbonates from northern Spain, *J. Geophys. Res.-Solid
1478 Earth*, 107(B4), 14–14, 2002.
- 1479 Weil, A. B., Gutiérrez-Alonso, G. and Conan, J.: New time constraints on lithospheric-scale
1480 oroclinal bending of the Ibero-Armorican Arc: a palaeomagnetic study of earliest Permian rocks
1481 from Iberia, *J. Geol. Soc.*, 167(1), 127–143, doi:10.1144/0016-76492009-002, 2010.
- 1482 Weil, A.B., Yonkee, A., and Sussman, A.: Reconstructing the kinematics of thrust sheet rotation:
1483 a paleomagnetic study of Triassic redbeds from the Wyoming Salient, U.S.A., *GSA Bulletin*,
1484 122, ½ 2-23, 2010.
- 1485 Weil, A. B. B., Gutiérrez-Alonso, G., Johnston, S. T. and Pastor-Galán, D.: Kinematic
1486 constraints on buckling a lithospheric-scale orocline along the northern margin of Gondwana: A
1487 geologic synthesis, *Tectonophysics*, 582, 25–49, doi:10.1016/j.tecto.2012.10.006, 2013.
- 1488 Woodcock, N. H., Soper, N. J. and Strachan, R. A.: A Rheic cause for the Acadian deformation
1489 in Europe, *J. Geol. Soc.*, 164, 1023–1036, 2007.
- 1490 Yenes, M., Alvarez, F. and Gutierrez-Alonso, G.: Granite emplacement in orogenic
1491 compressional conditions: the La Alberca-Bejar granitic area (Spanish Central System, Variscan
1492 Iberian Belt), *J. Struct. Geol.*, 21(10), 1419–1440, 1999.
- 1493 Yonkee, A., Weil, A.B., and Sussman, A.: Reconstructing the kinematic evolution of curved
1494 mountain belts: internal strain patterns in the Wyoming Salient, Sevier thrust belt, U.S.A., *GSA
1495 Bulletin*, 122, ½, 24-50, 2010.
- 1496 Yonkee, A. and Weil, A. B.: Quantifying vertical axis rotation in curved orogens: Correlating
1497 multiple data sets with a refined weighted least squares strike test, *Tectonics*, 29(3), 31 PP.-31
1498 PP., doi:10.1029/2008TC002312, 2010b.
- 1499 Zegers, T. E., Dekkers, M. J. and Bailly, S.: Late Carboniferous to Permian remagnetization of
1500 Devonian limestones in the Ardennes: Role of temperature, fluids, and deformation, *J. Geophys.
1501 Res. Solid Earth*, 108(B7), n/a-n/a, doi:10.1029/2002JB002213, 2003.

1502 Captions

1503 Fig. 1 Simplified paleogeographic map of the Variscan-Alleghanian orogeny prior to the
1504 Jurassic break-up of Pangea, with the major orogenic curves labeled. Note, this map represents
1505 Iberian outcrops without taking into account post-Jurassic Alpine deformation (see text for
1506 details e.g. Gong et al., 2008; Pastor-Galán et al., 2018). Slightly darker colors in the Variscan

1507 belt indicate present-day European and African outcrops (modified after Martínez-Catalán et al.,
1508 2009; Weil et al., 2013).

1509 Fig. 2 A) Present-day configuration of the tectonostratigraphic zones of the Iberian
1510 Variscides and their major structures. White areas represent Mesozoic and Cenozoic cover. B)
1511 Three competing geometric proposals for the Central Iberian curve. 1) A disharmonic curvature,
1512 up to 160° at the outer arc but much less pronounced at the inner arc (Aerden, 2004); 2) A
1513 harmonic, but more open curvature as suggested by Martínez Catalán (2012); 3) An isoclinal
1514 curvature model (Shaw et al., 2012). C) Distribution of the E1 (migmatitic domes) and C3 to
1515 post-C3 granitoids in the NW of Iberia (modified from Pastor-Galán et al., 2016)

1516 Fig. 3 A) Stratigraphic synthesis of the Gondwanan platform series in NW Iberia.
1517 Cantabrian Zone columns are after Aramburu et al., 2002; Bastida, 2004; Murphy et al 2008;
1518 Pastor-Galán et al., 2013a; 2013b. Iberian Range follows Gozalo et al., 2008; Mergl and
1519 Zamora, 2012 and Calvín and Casas, 2014. West Asturian-Leonese Zone stratigraphy is after
1520 Pérez-Estaún, 1990; Marcos, 2004; Martínez-Catalán et al., 2004a; Gutiérrez-Marco et al.,
1521 2019. Central Iberian Zone follows Díez-Balda, 1986; Valladares et al., 2000; Díez Montes,
1522 2007; Martínez-Catalán et al., 2004b; del Moral and Sarmiento, 2008; García-Arias et al., 2018.
1523 B) Ordovician paleocurrents orientations, modified from Shaw et al. (2012). C) Schematic basin
1524 architecture inferred from the stratigraphic compilation.

1525 Fig. 4 A) The kinematic evolution of the Cantabrian Orocline in its core, the Cantabrian
1526 Zone, inferred from total least squares (TLS) orocline tests (Pastor-Galán et al. 2017). B) Three
1527 orocline (strike) tests used to constrain the kinematics of the Cantabrian Orocline. The
1528 Ordovician paleocurrents, which predate any orogenic movement, recorded the complete
1529 vertical-axis rotation history and yields a slope (m) of ~ 1 . The Moscovian paleomagnetic data
1530 (from Weil et al., 2013; Pmag.), which postdates the main orogenic phases (C1, C2 and E1) and
1531 is coeval with C3, shows a slope of ~ 1 . The Gzhelian joint sets (from Pastor-Galán et al., 2011)
1532 orocline test shows a slope of ~ 0.5 , which indicates that part of the orocline was already formed
1533 between 304 Ma and 300 Ma.

1534 Fig. 5 A) Aeromagnetic map of Spain (Ardizzone et al., 1989, for Spain and the World
1535 Digital Magnetic Anomaly Map (WDMAM project) and Portugal (modified from Martínez Catalán,
1536 2012 and Martínez Catalán et al., 2015), showing the possible trace of the Central Iberian
1537 curve. B) Bouguer anomalies of the Iberian Peninsula, modified from Ayala et al., 2016. Gravity
1538 anomalies do not reflect the geometry of the Cantabrian Orocline nor the Central Iberian curve,
1539 but are related to the Cenozoic Alpine lithospheric structure.

1540 Fig. 6 Paleomagnetic studies related to the Cantabrian Orocline and the Central Iberian

1541 curve: (1) Synthesis of paleomagnetism in the core of the Cantabrian Orocline (see Weil et al.,
1542 2013); (2) Permian (eP) components synthesized in Weil et al. (2010); (3) Ordovician volcanics
1543 and limestones (Laquiama) in the boundary between the West Asturian-Leonese and Central
1544 Iberian Zones (Fernández-Lozano et al., 2016); (4) Devonian sedimentary sequences and
1545 Permian subvolcanics in the Iberian ranges (Pastor-Galán et al., 2018); (5) Permian dykes and
1546 sills (Calvín et al., 2014); (5) Anatectic granites (E1) and mantle derived granitoids (C3) from
1547 Tormes Dome and Central System (Pastor-Galán et al., 2016); (6) Cambrian limestones from
1548 Tamames (N) and los Navalucillos (S) (Pastor-Galán et al., 2015a); (7) Ediacaran-Early
1549 Cambrian sedimentary rocks in the southern sector of the Central Iberian Zone (Pastor-Galán et
1550 al., 2017b); (8) Almadén volcanics from the Central Iberian Zone (Perroud et al., 1991; Parés
1551 and van der Voo, 1992; Leite Mendes et al. in press) and Volcanic rocks from southern Ossa
1552 Morena and the South Portuguese Zone (Leite Mendes et al. in press)

1553 Fig. 7 Magnetization components with a positive reversal test in the extensional
1554 anatectic granites of Tormes (A) and Martinamor Domes (B). This component is interpreted as
1555 primary with a magnetization age of >318 Ma (Pastor-Galán et al., 2016). C) Distribution of
1556 directions and VGPs and statistical parameters from both domes combined.

1557 Fig. 8 Cartoon depicting the different vertical-axis rotation events that occurred in the
1558 Cantabrian Zone and the Iberian Range, modified from Pastor-Galán et al. (2018). (A) Original
1559 quasilinear Variscan Orogenic belt, B) Formation of the Cantabrian Orocline around the
1560 Carboniferous–Permian boundary after a $\sim 70^\circ$ counterclockwise rotation in the Southern branch
1561 of the Cantabrian Zone and the Iberian Range. This rotation matches the rotation for the
1562 Cantabrian Orocline, see the fit of the Iberian Range Component #2 in the orocline test for the
1563 Cantabrian Zone (below). C) Post-Permian (Cenozoic) rotation of $\sim 22^\circ$ clockwise (CW) likely
1564 produced by differential shortening during the Alpine orogeny (Izquierdo-Llavall et al., 2018).
1565 Below, the global magnetic polarity time-scale for the Pennsylvanian and Cisuralian (following
1566 Ogg et al., 2016). TLS = Total Least Squares. Note that once the 22° CW rotation in the Iberian
1567 Range is corrected, components #2, #1, and P fit as expected with the APWP for the southern
1568 limb of the Cantabrian Orocline (Pastor-Galán et al., 2016).

1569 Fig. 9 Compilation of the directional distributions and average declinations with
1570 parachute of confidence (Δ Declination) in sites around the Central Iberian curve (see Fig. 6).
1571 The results show general CCW rotations in contrast to the expected CW rotations if the Central
1572 Iberia curve formed by vertical-axis rotations (see text). Results are compared with the expected
1573 declinations if those sites were part of the Cantabrian Orocline following the methodology
1574 described in Pastor-Galán et al. (2017b).

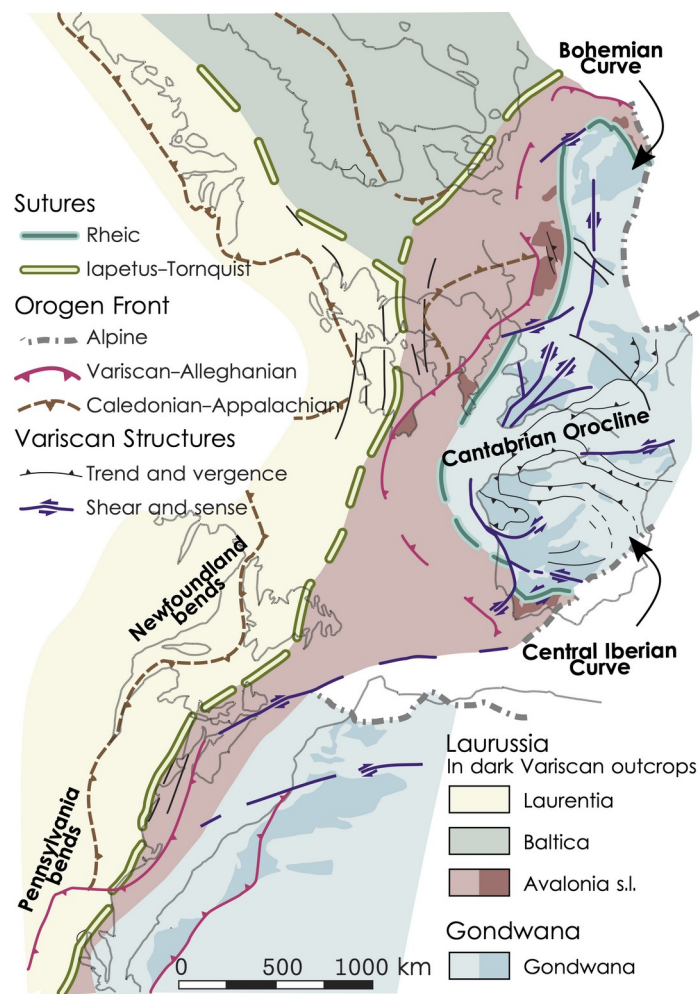
1575 Fig. 10 Orocline test of the Cantabrian Orocline (Weil et al., 2013) compared with the
1576 magnetizations found in the adjacent Laurussian segments of the orogen: Ireland (Pastor-Galán
1577 et al., 2015b) and the South Portuguese Zone (Leite Mendes et al., in press)

1578

1579 Fig. 11 Pioneering hypotheses for the Central Iberian curve. Note that none of them fulfill
1580 the most recent geometric and kinematic criteria. A) Simplified ribbon continent model after
1581 Johnston et al. (2013) and Shaw and Johnston (2016). B) Dextral mega-shear model from
1582 Martínez-Catalán (2011). C) Kinematic model with indentation and left-lateral shearing after
1583 Simancas et al. (2013)

1584 Fig. 12 Preliminary kinematic proposal for the Iberian Variscides. A) Pre-collisional stage
1585 after the opening of the Galicia Tras-os-Montes restricted seaway (e.g. Pin et al., 2002;
1586 Gutiérrez-Alonso et al., 2008a; Arenas et al., 2016). The irregular shape of the margin and the
1587 younging westwards deformation front (e.g. Daleyer et al., 1997) resulted in tectonic escape
1588 towards the still open Rheic Ocean (e.g. Braid et al., 2011; Murphy et al., 2016). B) After closure
1589 of the Rheic Ocean, C1 and C2 structures formed. The Galicia Tras-os-Montes was emplaced
1590 orogen parallel (e.g. Martínez-Catalán et al., 1990; Dias da Silva et al., 2020), preserving the
1591 shape of the seaway (i.e. a primary arc). C) The gravitational collapse of the orogen produced
1592 widespread anatexis and fold interference in the hinterland and the emplacement of the foreland
1593 fold-and-thrust belt. D) At Pennsylvanian times a change in the far-field stress buckled the
1594 Variscan belt around a vertical axis (see Gutiérrez-Alonso et al., 2008; Weil et al., 2013; Pastor-
1595 Galán et al., 2015a for details), creating new interference patterns and a lithospheric-scale
1596 response (see Gutiérrez-Alonso et al., 2004, 2011a; Pastor-Galán et al., 2012a). E) When the
1597 orocline became too tight to keep rotating, new cross-cutting brittle structures (C4) formed and
1598 minor extensional collapse (E2) occurred (e.g. Fernández-Lozano et al., 2019; Dias da Silva et
1599 al., 2020).

1600 Fig. 1 Simplified paleogeographic map of the Variscan-Alleghanian orogeny prior to the
 1601 Jurassic break-up of Pangea, with the major orogenic curves labeled. Note, this map represents
 1602 Iberian outcrops without taking into account post-Jurassic Alpine deformation (see text for
 1603 details e.g. Gong et al., 2008; Pastor-Galán et al., 2018). Slightly darker colors in the Variscan
 1604 belt indicate present-day European and African outcrops (modified after Martínez-Catalán et al.,
 1605 2009; Weil et al., 2013).



1606

1607

1608

1609

1610

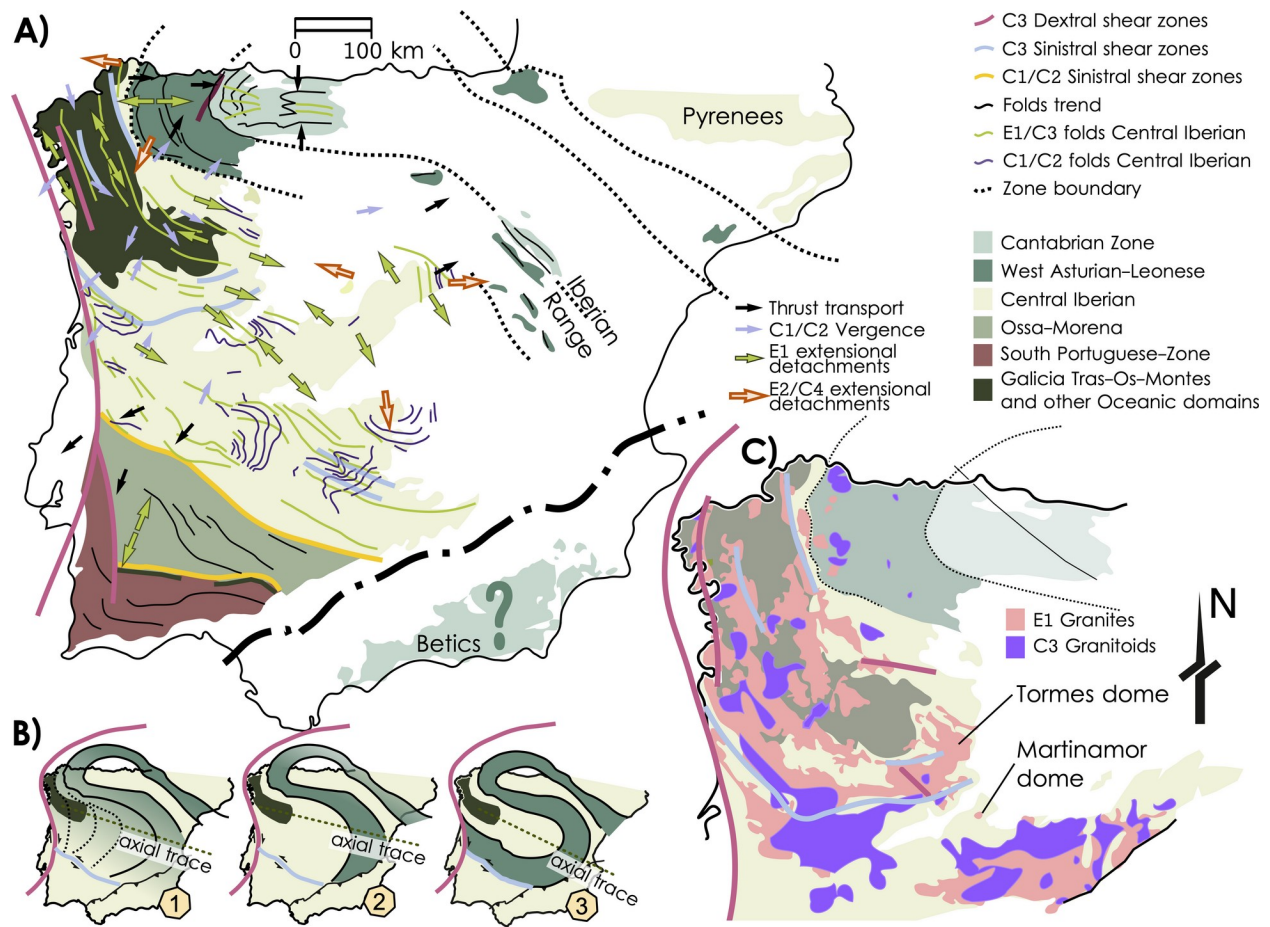
1611

1612

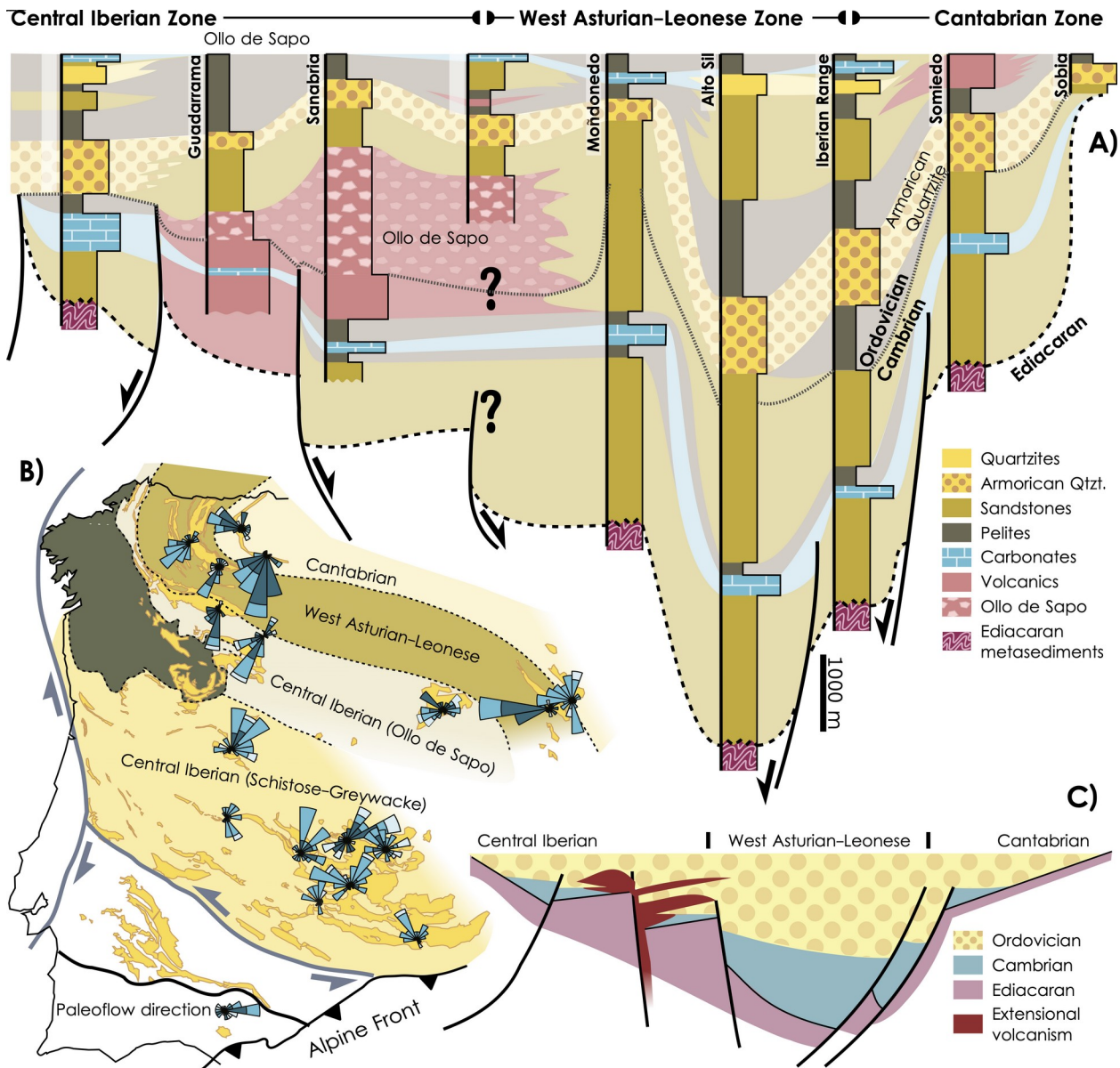
1613

1614

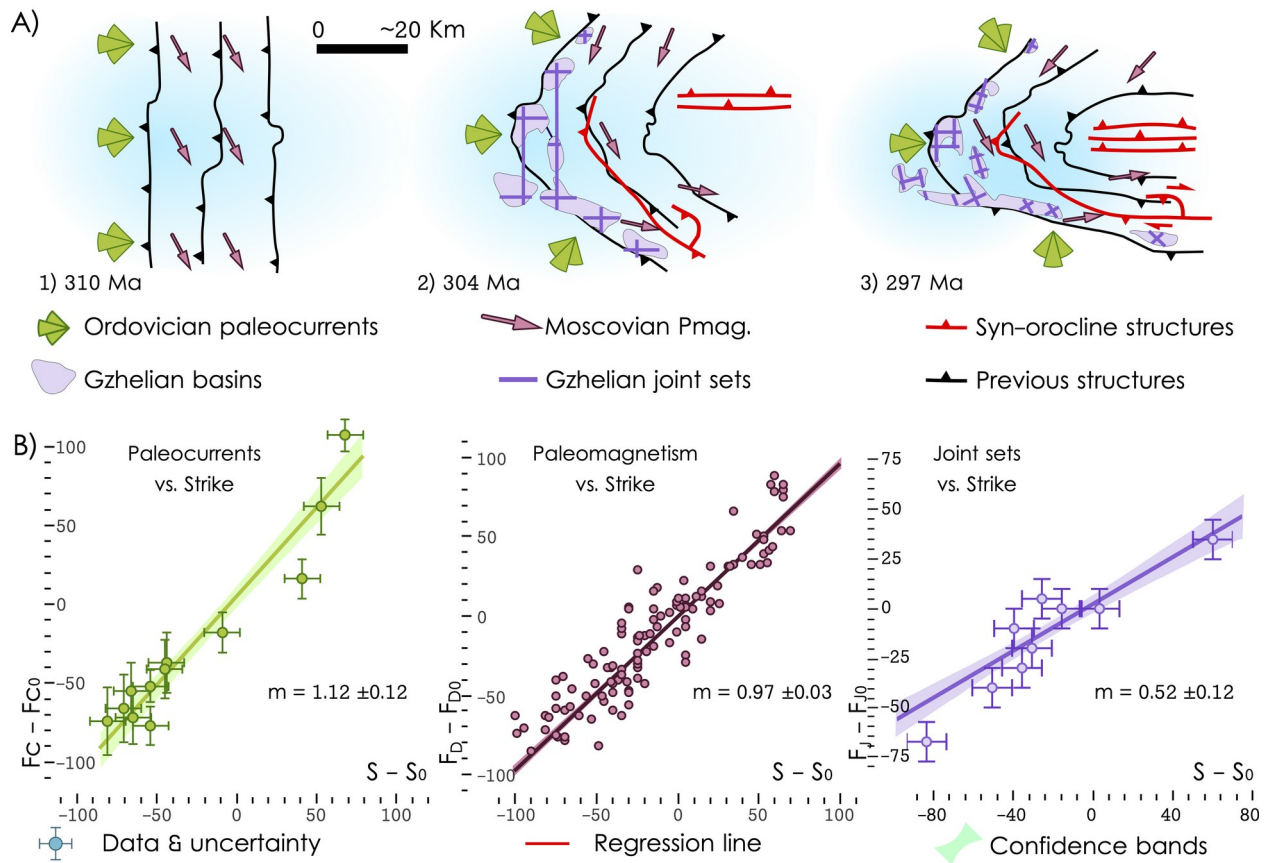
Fig. 2 A) Present-day configuration of the tectonostratigraphic zones of the Iberian Variscides and their major structures. White areas represent Mesozoic and Cenozoic cover. B) Three competing geometric proposals for the Central Iberian curve. 1) A disharmonic curvature, up to 160° at the outer arc but much less pronounced at the inner arc (Aerden, 2004); 2) A harmonic, but more open curvature as suggested by Martínez Catalán (2012); 3) An isoclinal curvature model (Shaw et al., 2012). C) Distribution of the E1 (migmatitic domes) and C3 to post-C3 granitoids in the NW of Iberia (modified from Pastor-Galán et al., 2016)



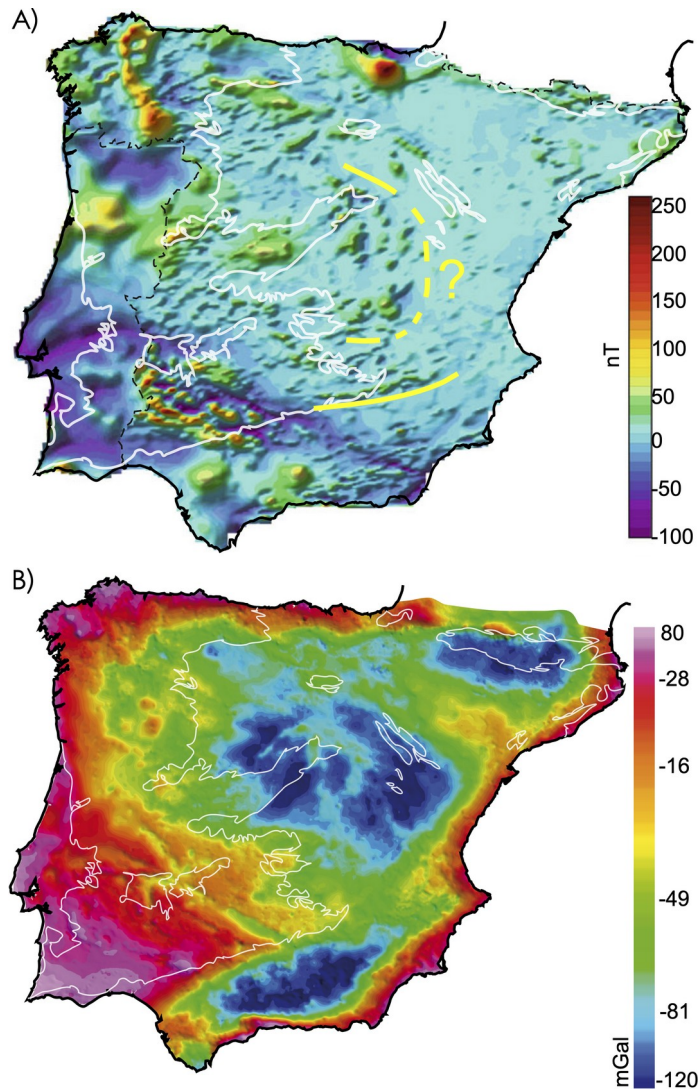
1615 Fig. 3 A) Stratigraphic synthesis of the Gondwanan platform series in NW Iberia.
 1616 Cantabrian Zone columns are after Aramburu et al., 2002; Bastida, 2004; Murphy et al 2008;
 1617 Pastor-Galán et al., 2013a; 2013b. Iberian Range follows Gozalo et al., 2008; Mergl and
 1618 Zamora, 2012 and Calvín and Casas, 2014. West Asturian-Leonese Zone stratigraphy is after
 1619 Pérez-Estaún, 1990; Marcos, 2004; Martínez-Catalán et al., 2004a; Gutiérrez-Marco et al.,
 1620 2019. Central Iberian Zone follows Díez-Balda, 1986; Valladares et al., 2000; Díez Montes,
 1621 2007; Martínez-Catalán et al., 2004b; del Moral and Sarmiento, 2008; García-Arias et al., 2018.
 1622 B) Ordovician paleocurrents orientations, modified from Shaw et al. (2012). C) Schematic basin
 1623 architecture inferred from the stratigraphic compilation.



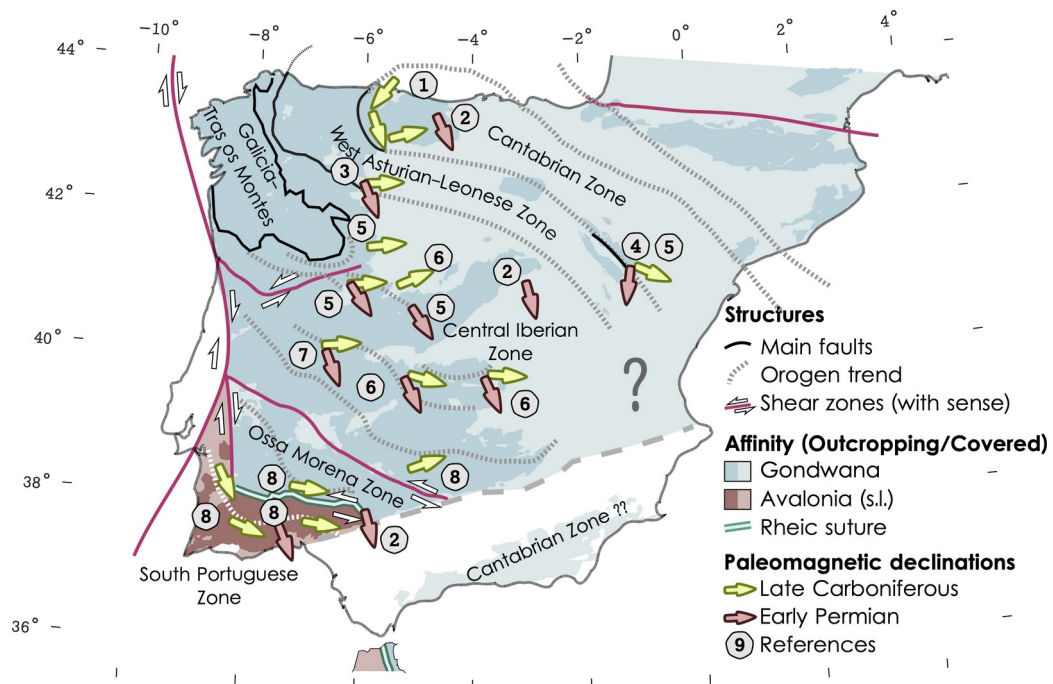
1625 Fig. 4 A) The kinematic evolution of the Cantabrian Orocline in its core, the Cantabrian
 1626 Zone, inferred from total least squares (TLS) orocline tests (Pastor-Galán et al. 2017). B) Three
 1627 orocline (strike) tests used to constrain the kinematics of the Cantabrian Orocline. The
 1628 Ordovician paleocurrents, which predate any orogenic movement, recorded the complete
 1629 vertical-axis rotation history and yields a slope (m) of ~1. The Moscovian paleomagnetic data
 1630 (from Weil et al., 2013; Pmag.), which postdates the main orogenic phases (C1, C2 and E1) and
 1631 is coeval with C3, shows a slope of ~1. The Gzhelian joint sets (from Pastor-Galán et al., 2011)
 1632 orocline test shows a slope of ~0.5, which indicates that part of the orocline was already formed
 1633 between 304 Ma and 300 Ma.



1635 Fig. 5 A) Aeromagnetic map of Spain (Ardizzone et al., 1989, for Spain and the World
1636 Digital Magnetic Anomaly Map (WDMAM project) and Portugal (modified from Martínez Catalán,
1637 2012 and Martínez Catalán et al., 2015), showing the possible trace of the Central Iberian
1638 curve. B) Bouguer anomalies of the Iberian Peninsula, modified from Ayala et al., 2016. Gravity
1639 anomalies do not reflect the geometry of the Cantabrian Orocline nor the Central Iberian curve,
1640 but are related to the Cenozoic Alpine lithospheric structure.
1641



1642 Fig. 6 Paleomagnetic studies related to the Cantabrian Orocline and the Central Iberian
 1643 curve: (1) Synthesis of paleomagnetism in the core of the Cantabrian Orocline (see Weil et al.,
 1644 2013); (2) Permian (eP) components synthesized in Weil et al. (2010); (3) Ordovician volcanics
 1645 and limestones (Laquiana) in the boundary between the West Asturian-Leonese and Central
 1646 Iberian Zones (Fernández-Lozano et al., 2016); (4) Devonian sedimentary sequences and
 1647 Permian subvolcanics in the Iberian ranges (Pastor-Galán et al., 2018); (5) Permian dykes and
 1648 sills (Calvín et al, 2014); (5) Anatectic granites (E1) and mantle derived granitoids (C3) from
 1649 Tormes Dome and Central System (Pastor-Galán et al., 2016); (6) Cambrian limestones from
 1650 Tamames (N) and los Navalucillos (S) (Pastor-Galán et al., 2015a); (7) Ediacaran-Early
 1651 Cambrian sedimentary rocks in the southern sector of the Central Iberian Zone (Pastor-Galán et
 1652 al., 2017b); (8) Almadén volcanics from the Central Iberian Zone (Perroud et al., 1991; Parés
 1653 and van der Voo, 1992; Leite Mendes et al. in press) and Volcanic rocks from southern Ossa
 1654 Morena and the South Portuguese Zone (Leite Mendes et al, in press)



1655

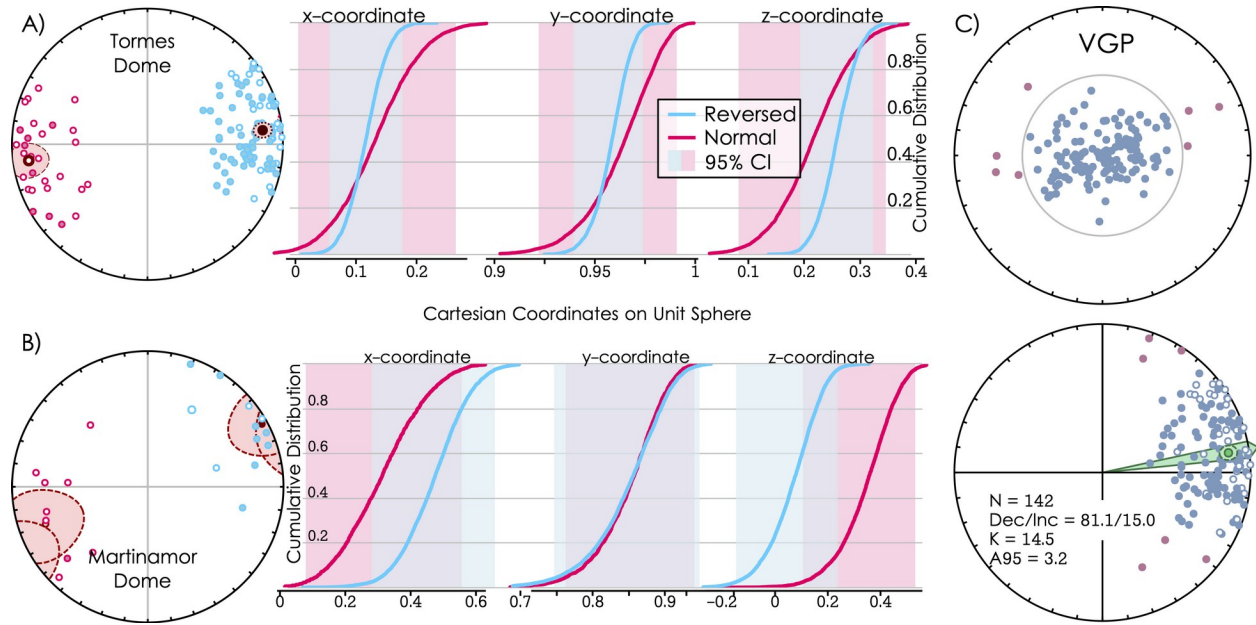
1656

1657

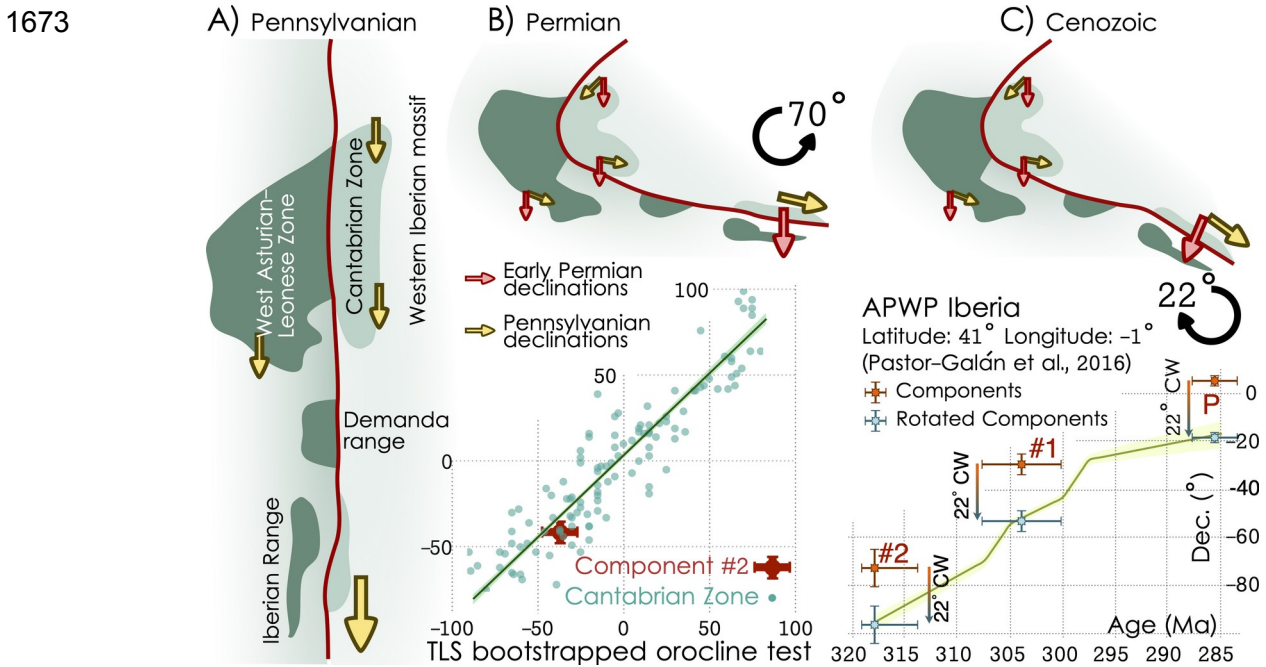
1658

1659

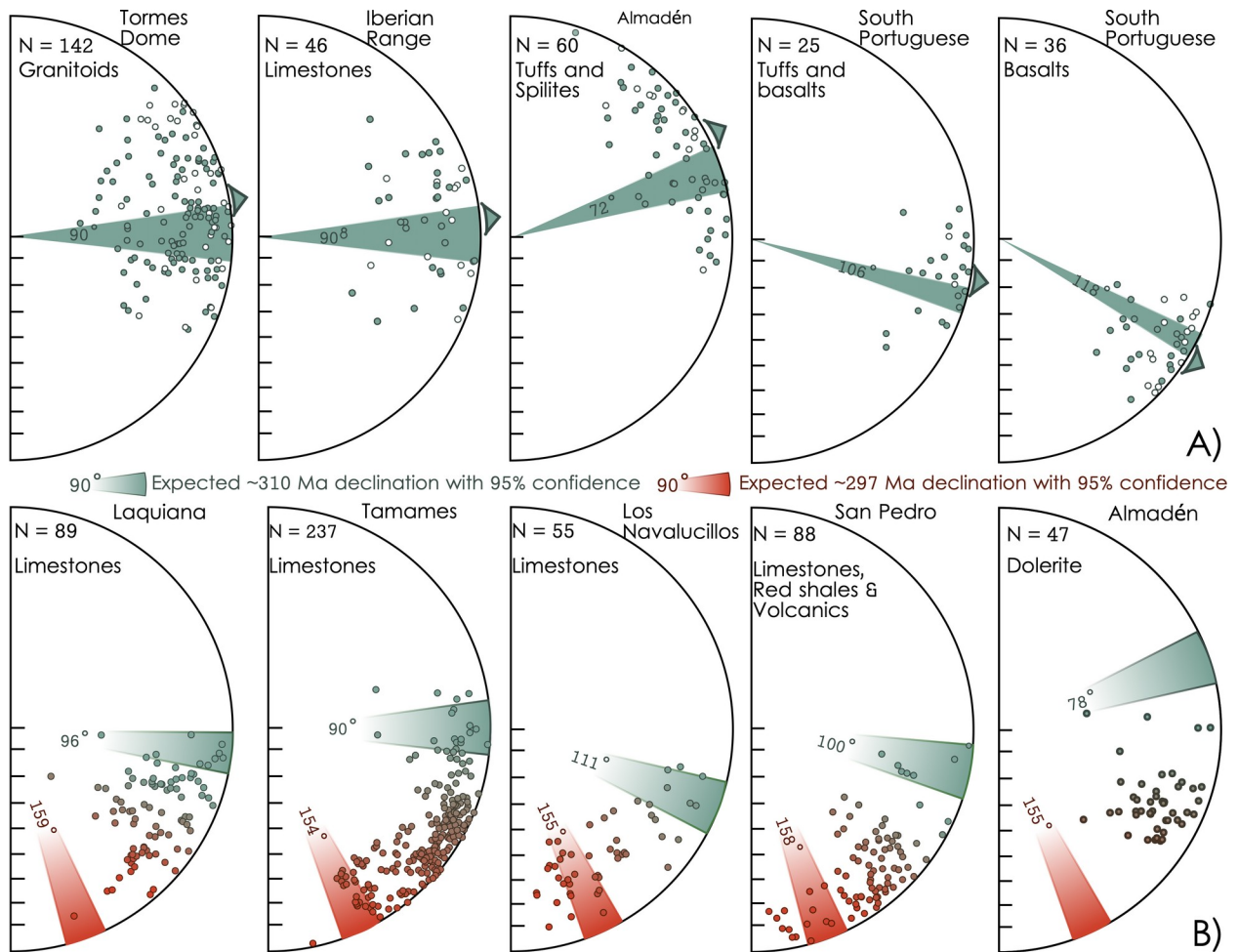
Fig. 7 Magnetization components with a positive reversal test in the extensional anatectic granites of Tormes (A) and Martinamor Domes (B). This component is interpreted as primary with a magnetization age of >318 Ma (Pastor-Galán et al., 2016). C) Distribution of directions and VGPs and statistical parameters from both domes combined.



1661 Fig. 8 Cartoon depicting the different vertical-axis rotation events that occurred in the
 1662 Cantabrian Zone and the Iberian Range, modified from Pastor-Galán et al. (2018). (A) Original
 1663 quasilinear Variscan Orogenic belt, B) Formation of the Cantabrian Orocline around the
 1664 Carboniferous–Permian boundary after a $\sim 70^\circ$ counterclockwise rotation in the Southern branch
 1665 of the Cantabrian Zone and the Iberian Range. This rotation matches the rotation for the
 1666 Cantabrian Orocline, see the fit of the Iberian Range Component #2 in the orocline test for the
 1667 Cantabrian Zone (below). C) Post-Permian (Cenozoic) rotation of $\sim 22^\circ$ clockwise (CW) likely
 1668 produced by differential shortening during the Alpine orogeny (Izquierdo-Llavall et al., 2018).
 1669 Below, the global magnetic polarity time-scale for the Pennsylvanian and Cisuralian (following
 1670 Ogg et al., 2016). TLS = Total Least Squares. Note that once the 22° CW rotation in the Iberian
 1671 Range is corrected, components #2, #1, and P fit as expected with the APWP for the southern
 1672 limb of the Cantabrian Orocline (Pastor-Galán et al., 2016).

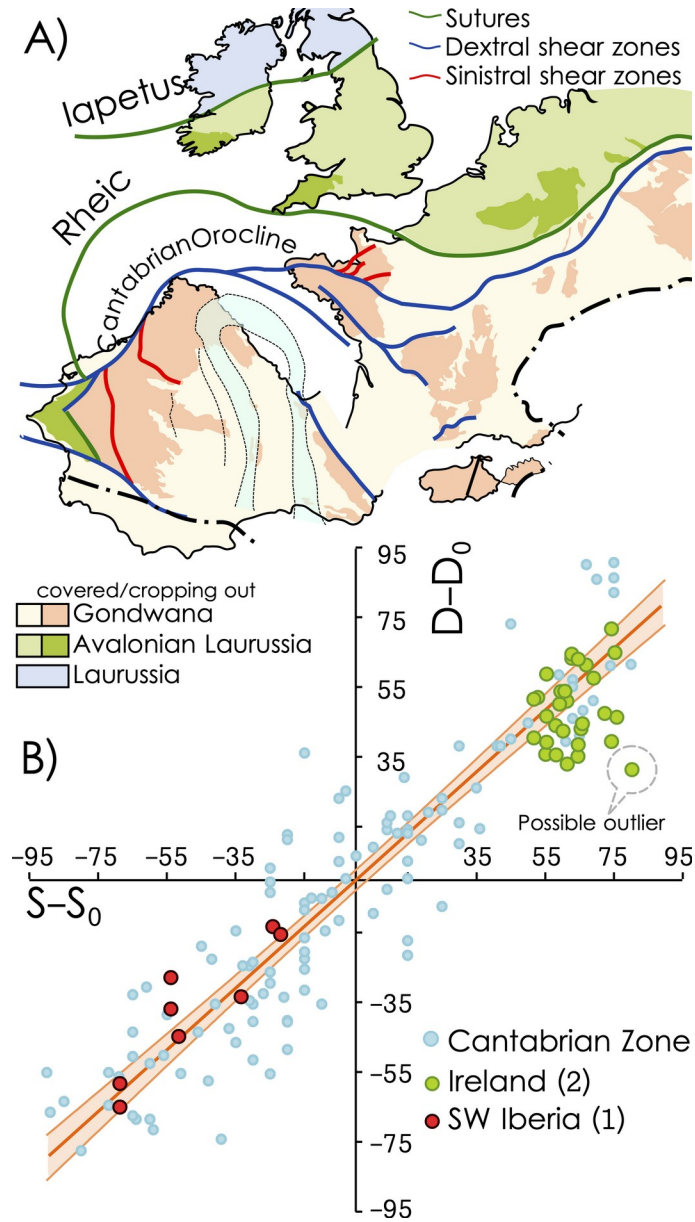


1674 Fig. 9 Compilation of the directional distributions and average declinations with
 1675 parachute of confidence (Δ Declination) in sites around the Central Iberian curve (see Fig. 6).
 1676 The results show general CCW rotations in contrast to the expected CW rotations if the Central
 1677 Iberia curve formed by vertical-axis rotations (see text). Results are compared with the expected
 1678 declinations if those sites were part of the Cantabrian Orocline following the methodology
 1679 described in Pastor-Galán et al. (2017b).

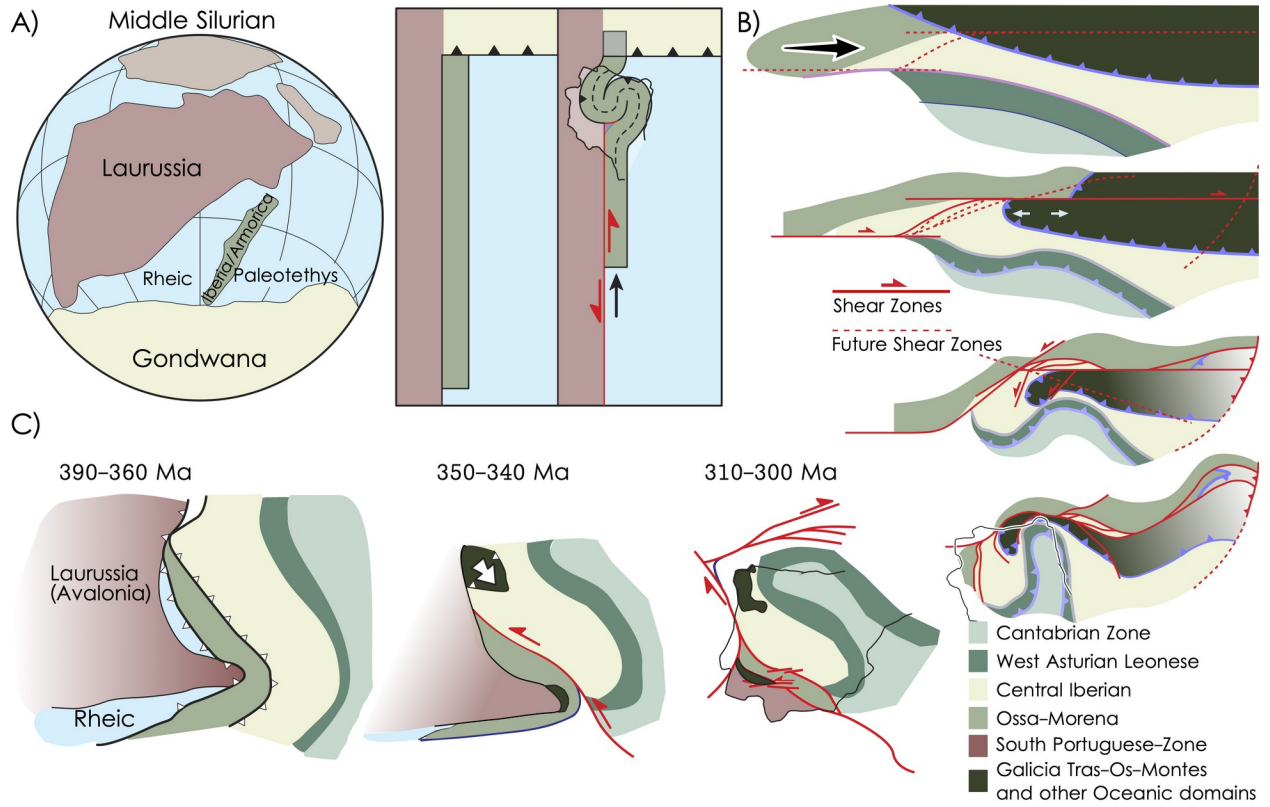


1681 Fig. 10 Orocline test of the Cantabrian Orocline (Weil et al., 2013) compared with the
 1682 magnetizations found in the adjacent Laurussian segments of the orogen: Ireland (Pastor-Galán
 1683 et al., 2015b) and the South Portuguese Zone (Leite Mendes et al., in press)

1684
 1685

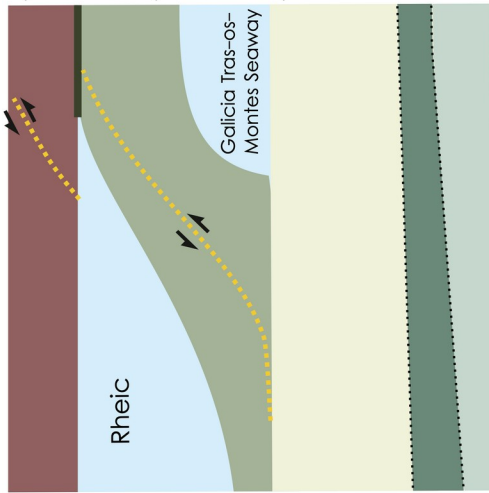


1686 Fig. 11 Pioneering hypotheses for the Central Iberian curve. Note that none of them fulfill
 1687 the most recent geometric and kinematic criteria. A) Simplified ribbon continent model after
 1688 Johnston et al. (2013) and Shaw and Johnston (2016). B) Dextral mega-shear model from
 1689 Martínez-Catalán (2011). C) Kinematic model with indentation and left-lateral shearing after
 1690 Simancas et al. (2013)

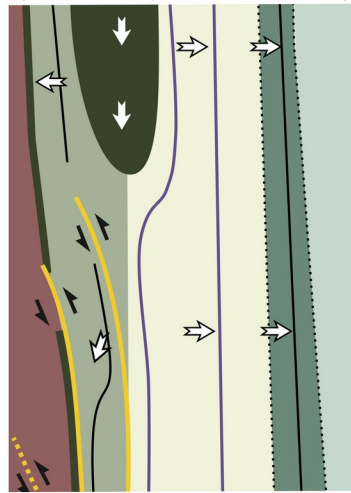


1692 Fig. 12 Preliminary kinematic proposal for the Iberian Variscides. A) Pre-collisional stage
1693 after the opening of the Galicia Tras-os-Montes restricted seaway (e.g. Pin et al., 2002;
1694 Gutiérrez-Alonso et al., 2008a; Arenas et al., 2016). The irregular shape of the margin and the
1695 younging westwards deformation front (e.g. Daleyer et al., 1997) resulted in tectonic escape
1696 towards the still open Rheic Ocean (e.g. Braid et al., 2011; Murphy et al., 2016). B) After closure
1697 of the Rheic Ocean, C1 and C2 structures formed. The Galicia Tras-os-Montes was emplaced
1698 orogen parallel (e.g. Martínez-Catalán et al., 1990; Dias da Silva et al., 2020), preserving the
1699 shape of the seaway (i.e. a primary arc). C) The gravitational collapse of the orogen produced
1700 widespread anatexis and fold interference in the hinterland and the emplacement of the foreland
1701 fold-and-thrust belt. D) At Pennsylvanian times a change in the far-field stress buckled the
1702 Variscan belt around a vertical axis (see Gutiérrez-Alonso et al., 2008; Weil et al., 2013; Pastor-
1703 Galán et al., 2015a for details), creating new interference patterns and a lithospheric-scale
1704 response (see Gutiérrez-Alonso et al., 2004, 2011a; Pastor-Galán et al., 2012a). E) When the
1705 orocline became too tight to keep rotating, new cross-cutting brittle structures (C4) formed and
1706 minor extensional collapse (E2) occurred (e.g. Fernández-Lozano et al., 2019; Dias da Silva et
1707 al., 2020).

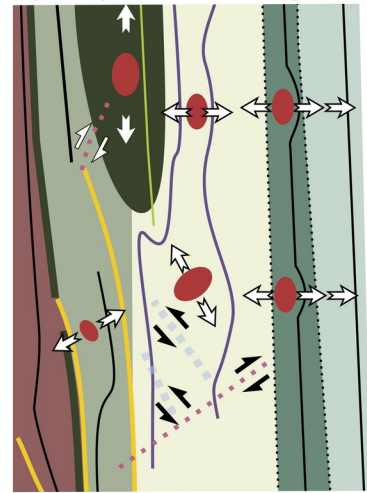
A) Pre C1 (~380 Ma)



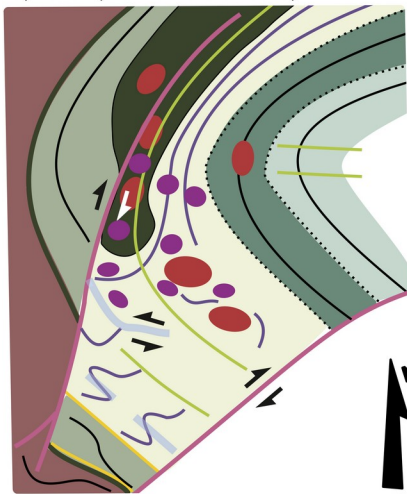
B) C1-C2 (~360-335 Ma)



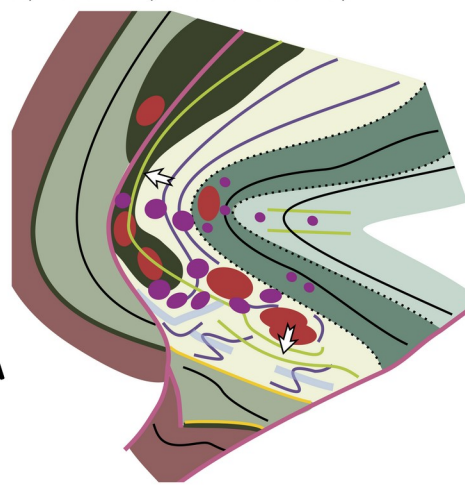
C) E1 (~330-317 Ma)



D) C3 (~315-300 Ma)



E) C4-E2 (~300-280 Ma)



- █ Cantabrian Zone
 - █ West Asturian-Leonese
 - █ Central Iberian
 - █ Ossa-Morena
 - █ South Portuguese-Zone
 - █ Galicia Tras-Os-Montes and other Oceanic domains
 - █ E1/E2 gneiss domes & granites
 - █ C3-C4 mantle derived granitoids
-
- C3 Dextral shear zones
 - C3 Sinistral shear zones
 - C1/C2 Sinistral shear zones
 - ~ Folds trend
 - ~ E1/C3 folds Central Iberian
 - ~ C1/C2 folds Central Iberian
 - ... Zone boundary
 - ↔ Transport direction